TROPICAL DATA ASSIMILATION AND ANALYSIS OF DIVERGENCE

P. Undén
European Centre for Medium Range Weather Forecasts,
Reading, Berkshire RG2 9AX, England

ABSTRACT

One of the major weaknesses of the ECMWF tropical analyses has been in the analysis of divergent wind due to the use of a non-divergent constraint on the wind components. It is possible to relax this traditional constraint in optimum interpolation analysis schemes and allow explicitly for divergent wind increments in the analysis. This has now been done in the ECMWF scheme and it is shown in this paper that there is a strong response to divergent signals in the observations even when only a small portion of divergence is included in the statistical model of the wind forecast errors. Wind observations are analysed more faithfully and tropical features appear more realistic with the divergent formulation. The previous non-divergent ECMWF analysis scheme still provided divergence on larger scales but on the smallest scales the resulting analysis increments of divergence displayed mainly noise. This disappears with the explicit inclusion of divergence and the divergence increments become smooth and coherent. Three different vertical correlation functions for the velocity potential have been tried out but none of them is able to enhance vertical velocities and tropical convection to any significant degree when using single level data alone. Tests in data assimilations show that the divergent analyses fit wind data consistently better but medium range forecasts from these assimilations are little affected by the improved analyses.

1. INTRODUCTION

The ECMWF mass and wind analysis uses a multi-variate optimum interpolation (OI) scheme (Lorenc (1981)). Observed heights, pressures, wind components and thicknesses are used simultaneously to analyse surface pressure, heights and wind components on the model's Gaussian grid (and levels). As a first guess for the analysis a 6 hour forecast from the previous analysis is used and it is the differences between the observations and this first guess which are analysed. The degree to which data are fitted is controlled by some of the statistical properties of the first guess errors and observation errors. These are not known a priori but are modelled based on representative

statistics accumulated at ECMWF (see Hollingsworth and Lonnberg (1986) and Lonnberg and Hollingsworth (1986)).

The statistics are not only used to interpolate observed differences to gridpoints but they also have an important role in the filtering of the observed departures from the first guess. Standard deviations of first guess and observation errors determine the relative weights between the first guess and the observations. The spatial correlation functions (also referred to as structure functions) filter out observed information which is not desired, e.g. random errors and motion on scales which are not resolved by the forecast model. Cross-correlations between heights and winds define the degree of geostrophy in the analysis.

The cross-correlations between u- and v-components of the wind have, until recently, been based on a non-divergent statistical model of the wind forecast errors. This would make the resulting analysed departures from the first guess field (analysis increments) non-divergent everywhere, if all the data from the whole globe were analysed simultaneously. Since this is not possible to achieve in practice, non-divergence can only be ensured locally inside one analysis volume. At ECMWF these volumes are in the form of "boxes" where all observations in the box and its immediate surroundings are used to analyse the model variables at all the gridpoints in this volume. The sizes of the boxes are approximately 625 by 625 km in the horizontal (or less in very data dense areas). In the vertical the volume is divided into two slabs (surface - 100 hPa and 300 - 10 hPa). It is through this simultaneous use of observations that the filtering takes place and it is inside each box volume that the analysis increments obey the relationships imposed by the statistical models (e.g. near geostrophy and non-divergence). Neighbouring boxes, however, do normally not use exactly the same set of observations and it is likely to be some inconsistencies between the analyses in different boxes. Smooth transitions of the analysis increments are ensured through analysing gridpoints in the border zones of the boxes also from neighbouring boxes and averaging the values with weights depending on distance from box centres. This procedure does not, however, guarantee that their spatial derivatives also are smooth.

With the non-divergent statistical model the analysis increments still contain divergence on larger scales due to the different, albeit locally non-divergent, winds in the different boxes. On scales smaller than the box scale the divergence is, however, largely spurious and "noisy" when e.g. calculated across a box boundary. It will be showed in Section 4 that this noise problem is largely eliminated when a partly divergent model for the wind forecast errors is introduced. Since the ECMWF analysis system allows for the large scales of divergence but not the small scales it would be consistent to allow for divergence explicitly inside the box volumes by relaxing the non-divergent constraint.

The main reason for introducing divergent structure functions in the ECMWF analysis system is of course to be able to analyse divergent wind observations directly. The tropical analyses with the previous non-divergent scheme could be quite unrealistic since strongly divergent wind data were hardly drawn to at all. This has often been observed operationally at ECMWF and an example of such a case is shown in Section 4. Also examinations of FGGE analyses revealed deficiencies in the analysis of tropical wind data related to the non-divergent constraint. Relaxation of this constraint was stated as a strong recommendation in National Research Council (1985).

Daley (1983) and (1985) derived a complete prediction error model in terms of geopotential, streamfunction and velocity potential but still limiting correlations to be homogeneous and isotropic. The extension of this formalism to allow also for an-isotropy has been discussed by Hollingsworth and Lonnberg (1986). Daley investigated the effects on two-dimensional analyses of cross-correlations between geopotential, streamfunction and velocity potential. Reducing the geostrophic coupling between geopotential and streamfunction and the coupling between the wind components through the non-divergent constraint gave a very nonlinear response in terms of analysis weights. He also simulated the ECMWF box analysis in two dimensions and showed that quite reasonable analyses could be obtained with even only a relatively small divergent part in the wind prediction error correlations.

A velocity potential prediction error model has been introduced in the ECMWF analysis system along the lines of Daley (1985) but formulated in natural coordinates on the sphere as explained in Section 2. The choice of values of

parameters and of structure functions, both horizontal and vertical, for the velocity potential error is discussed in Section 3. The most important results are demonstrated in Section 4 as they become apparent for just a single analysis of a case when the non-divergent analysis performed badly. The new scheme has been tried out in data assimilations with subsequent 10-day forecasts for two periods. The results are discussed in Sections 5 and 6. In the vertical the divergent part of the structure is not well known or easily determined so three different formulations have been tried during these assimilations. Also the impact of using a larger horizontal scale for the divergent forecast errors than for the non-divergent ones has been evaluated and is mentioned in section 6.

2. THE FORMALISM OF INCLUDING DIVERGENCE IN THE ANALYSIS

The OI-expression for the normalised analysis increment at a point is

$$a = \underline{p}^t \, (\underline{\underline{P}}+\underline{\underline{O}})^{-1} \, \underline{d} \qquad (2.1)$$

where the matrices $\underline{\underline{P}}$ and $\underline{\underline{O}}$ contain the prediction error and observation error correlations between observed data respectively. The vector $\underline{p}$ holds the correlations between the observed data and the datum to be analysed and the vector $\underline{d}$ contains the normalised observed data. Both the matrix $\underline{\underline{P}}$ and the vector $\underline{p}$ contain auto-correlations, e.g. z-z, u-u and v-v, for height and wind components as well as cross-correlations like z-u and u-v. All these quantities are best derived from a model of prediction error covariances of geopotential, streamfunction and velocity potential (and their cross-covariances) following Daley (1985).

$$\langle \phi\phi \rangle = E_\phi^2 \, V_\phi \, F(r) \qquad (2.2a)$$

$$\langle \psi\psi \rangle = E_\psi^2 \, V_\psi \, F(r) \qquad (2.2b)$$

$$\langle \chi\chi \rangle = E_\chi^2 \, V_\chi \, G(r) \qquad (2.2c)$$

$$\langle \phi\psi \rangle = \mu \, E_\phi E_\psi \, V_{\phi\psi} \, F(r) \qquad (2.2d)$$

$$\langle \chi\psi \rangle = 0 \qquad (2.2e)$$

$$\langle \chi\phi \rangle = 0 \qquad (2.2f)$$

Here homogenity and isotropy have been assumed since there is no angular and spatial dependence in the functions F and G. The geopotential and

streamfunction covariances have been assigned the same horizontal structure F(r) in order to facilitate the geostrophic constraint for the analysis via the geostrophic coupling constant my in (2.2d). A further simplification is that the cross-covariances between velocity potential and streamfunction as well as between velocity potential and geopotential have been set to zero since there is evidence that these terms are very small (see e.g. Hollingsworth and Lonnberg (1986) hereafter referred to as just HL). The prediction error covariance model has been assumed to be separable in one horizontal part (F and G) and another vertical part described by the various functions V above. The total wind prediction error variance E_ν^2 is divided into a divergent part (ν) and non-divergent part ($1-\nu$).

$$E_v^2 = E_\psi^2 + E_\chi^2 \tag{2.3a}$$

$$E_\chi^2 = \nu \; E_v^2 \tag{2.3b}$$

$$E_\psi^2 = (1-\nu) \; E_v^2 \tag{2.3c}$$

The horizontal wind covariances can then be derived by differentiating the streamfunction and velocity potential covariances using Helmholtz's theorem :

$$\underline{v} = \nabla\chi + \underline{k}.\nabla\psi \tag{2.4}$$

Using (2.4) will then give the correlations for the two components in terms of covariances of streamfunction and velocity potential in (2.2), assuming there is no horizontal variation in the error variances. In the ECMWF analysis system natural coordinates are employed where one longitudinal axis is along the direction of a line connecting the two points of interest and the other transverse axis is perpendicular to that line (Buell (1972), Lorenc (1981) and HL). The horizontal correlations between the wind components in this system at two points separated by a distance r are then

$$\langle u_l u_l \rangle = -(1-\nu) \frac{1}{r} V_\psi \frac{\partial F}{\partial r} - \nu V_\chi \frac{\partial^2 G}{\partial r^2} \tag{2.5}$$

$$\langle u_t u_t \rangle = -(1-\nu) V_\psi \frac{\partial^2 F}{\partial r^2} - \nu \frac{1}{r} V_\chi \frac{\partial G}{\partial r} \tag{2.6}$$

$$\langle u_l u_t \rangle = 0 \tag{2.7}$$

The correlations between wind components at any two points on the sphere can be computed by projecting the components in the local Cartesian coordinate systems on to the longitudinal and transverse directions (relative to the connecting line) and combining the two contributions from (2.5) and (2.6).

Also the height-wind correlation is affected by the partition of the wind variance into a correlated rotational part and a non-correlated divergent one.

$$\langle u_t z\rangle = -\langle z u_t\rangle = -\mu\, V_{\phi\psi}\, \sqrt{(1-\nu)}\, \frac{\partial F}{\partial r} \tag{2.8}$$

$$\langle u_l z\rangle = \langle z u_l\rangle = 0 \tag{2.9}$$

The height auto-correlation is still

$$\langle zz\rangle = V_\phi F \tag{2.10}$$

One can thus analyse also the divergent components of the winds by including the divergent terms in Eq. (2.5) and (2.6) for all the computations of wind correlations in the analysis as well as taking the altered normalisation into account in Eq. (2.5), (2.6) and (2.8).

The effect on the wind correlations of increasing the divergent part of the wind forecast error can be seen in Figs. 1 and 2 (the same horizontal scale is employed for both stream function and velocity potential). They display the vector and scalar correlations with a single u-component situated at 40°N, 40°W. The correlations are exactly as they would be in the ECMWF analysis system with full spherical geometry employed, except that the constant large scale term (see HL) is omitted for clarity. The v-v correlations are not shown here; they can be found by just rotating the u-u correlations 90 degrees anti-clockwise (apart from some change in shape due to map factors) and the v-u correlation is always the same as u-v as can be deduced from Eqs. (2.5) and (2.6). As ny is introduced with a value of 0.1 the major effect is to reduce the cross-correlation u-v and the negative lobes of the u-u correlation. The combined effect for the vectors is a significantly reduced return flow as the top panels in Fig. 1 show. When ny=0.5 the auto-correlation becomes circular (Fig. 2) and the cross-correlation zero since the longitudinal and transverse correlations now are equal ((2.5)

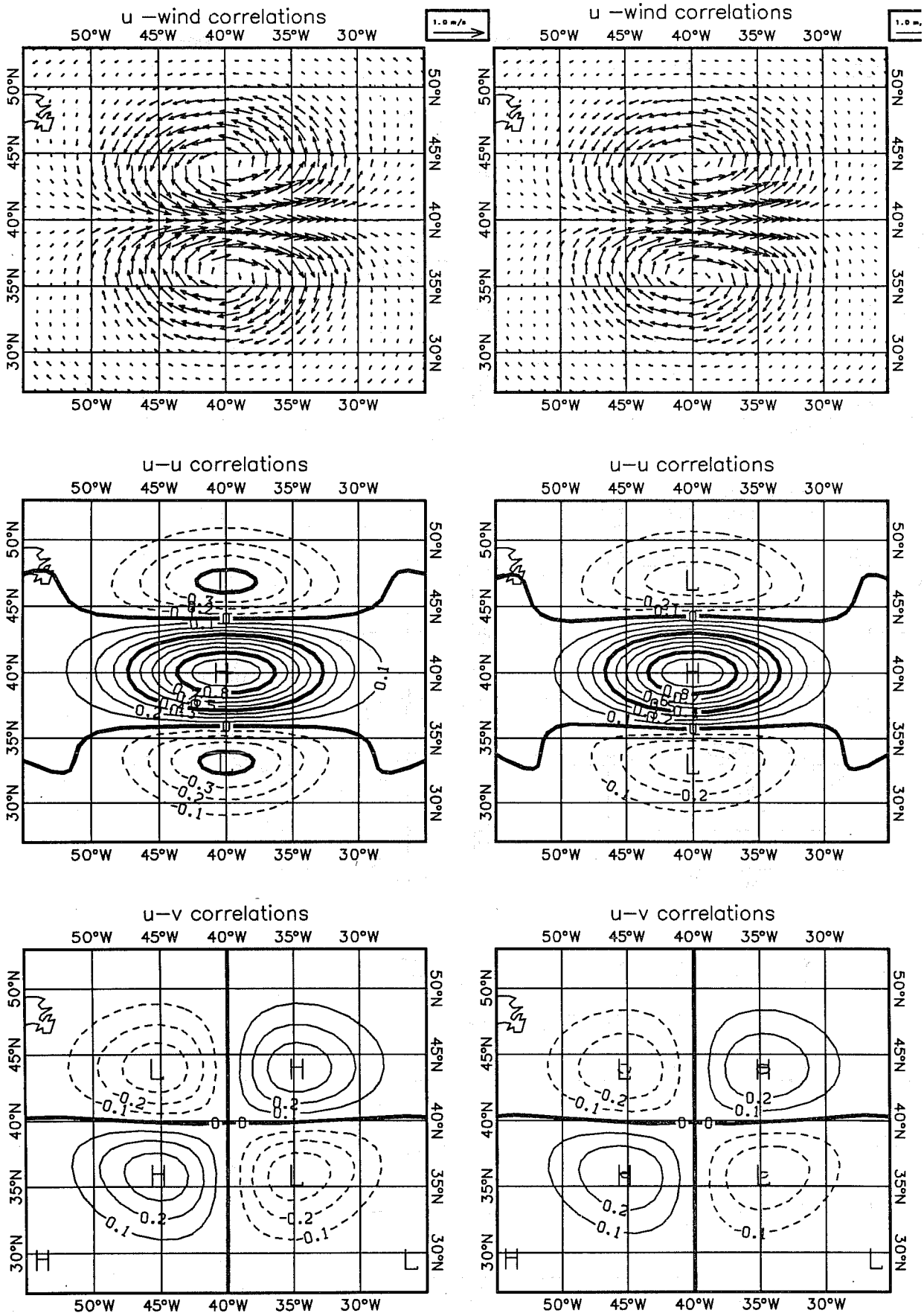

Figure 1. Horizontal correlations between a u wind component at 40°N, 40°W and wind vectors, u and v components for ν=0 (left) and ν=0.1 (right).

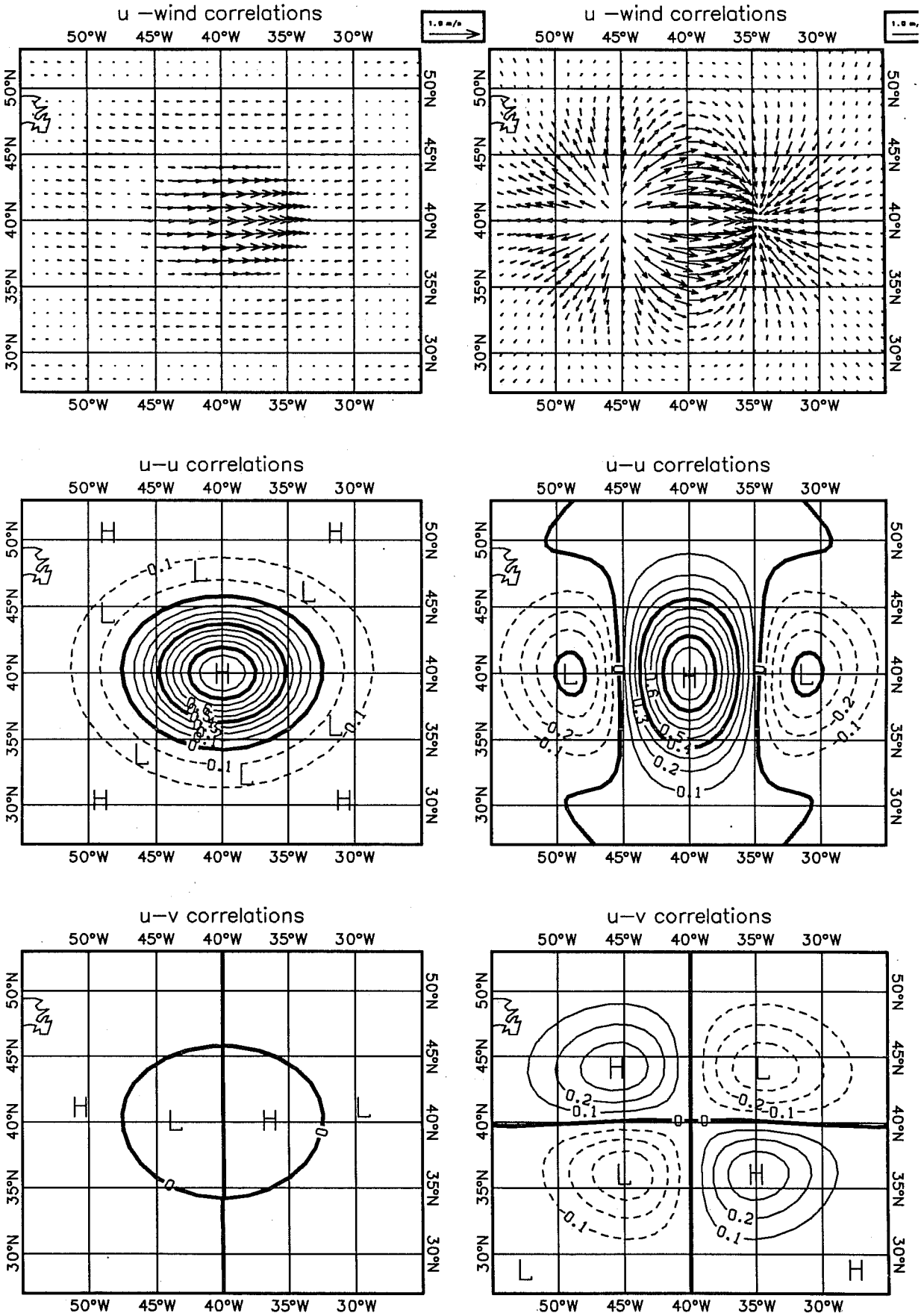

Figure 2. As Fig. 1 but for ν=0.5 (left) and ν=1.0 (right).

and(2.6)). (This is of course only true when the same horizontal structures F and G have been employed). With this choice of ny the analysis would be uni-variate in u and v and the definition of ny (2.3 a-c) implies that equal amounts of vorticity and divergence are assumed for the first guess error. Lorenc (1979) pointed out this consequence of analysing u and v components separately (univariate OI). Pedder (1988) has elaborated further on this subject and shown that univariate OI is likely to overestimate the divergence by a factor of the order of 2. Finally, when using purely divergent structure functions with ν=1 (Fig. 2 right) we see that the u-u and u-v correlations are of the same shape as for the non-divergent case but they are turned anti-clockwise 90 degrees.

3. PARAMETERIZATION OF THE DIVERGENT STRUCTURE FUNCTIONS

There are three parameters and functions available for controlling the divergence in the analysis ; the divergent part of the wind prediction error (ν), the vertical structure function (V_χ) and the horizontal structure function (G). These should ideally be chosen to agree as well as possible with what can be deduced from statistical knowledge of the forecast errors (e.g. as in HL). These are, however, only possible to determine to a certain accuracy and the results will not be optimal for all areas and weather situations. Structure functions have to be modelled as to agree reasonably well with the statistical results but with the strong constraint that the resulting correlation matrices should always be positive definite. Finally the performance of the formulations has to be evaluated in the context of analysis and data assimilation.

Daley (1985 and 1983) did not address the vertical problem and for the horizontal problem he concentrated on the sensitivity of the OI-analysis to the cross-correlations between the basic variables. He found that the response in terms of analysis weights is very non-linear as the divergent part of the wind error (ν) is increased from zero. The major part of the response takes place as ny increases to 0.1 and further increases have much smaller effects. An increase of ν also means a decrease of the cross-correlations between the wind components and the initial such decrease has the largest effect. A similar non-linear response was found also when the geostrophic coupling between geopotential and streamfunction was reduced from 1. Based on this argument and an investigation of analysis minus first guess fields at

ECMWF by Arpe (1982, pers.comm.) Daley (1983) found that 0.1 was a reasonable value for ν.

Another way of showing the analysis response is by eigenvector decomposition of the prediction error correlation matrix as described by Daley (1985) and in more detail by Hollingsworth (1984). The OI-analysis equation (2.1) can be used not only to analyse at grid points but also at the observation points. It then becomes:

$$\underline{a} = \underline{\underline{P}}^t \, (\underline{\underline{P}}+\underline{\underline{O}})^{-1} \, \underline{d} \tag{3.1}$$

Since the analysis is at observation points, the two $\underline{\underline{P}}$-matrices in (3.1) are identical. The result ($\underline{a}$) is a vector of analysis values for all analysis variables and observation points. The aim of this exercise is to find how much of the observations, $\underline{d}$, are retained by the analysis. This can of course be computed straight away for certain signatures in the observations and a range of observation errors. The advantage of the eigenvector decomposition is that a minimal number of orthogonal observation signatures (the eigenvectors) are obtained and that the dependence on the observation errors can be treated separately under some assumptions.

The $\underline{\underline{P}}$-matrix is decomposed into eigenvectors and eigenvalues:

$$\underline{\underline{P}} = \underline{\underline{E}} \, [\lambda] \, \underline{\underline{E}}^t \tag{3.2}$$

where $[\lambda]$ is a diagonal matrix of eigenvalues. To simplify matters the observation error correlation matrix is reduced to a diagonal matrix where all elements are σ^2. This is not too restrictive if we are considering the same type of observations in an area where the first guess forecast is of uniform quality.

$$\underline{\underline{O}} = \sigma^2 \, \underline{\underline{I}} \tag{3.3}$$

The $\underline{\underline{P}}+\underline{\underline{O}}$ matrix is then:

$$\underline{\underline{P}}+\underline{\underline{O}} = \underline{\underline{E}} \, [\lambda] \, \underline{\underline{E}}^t + \sigma^2 \, \underline{\underline{I}} \tag{3.4}$$

The inverse of this matrix is:

$$(\underline{\underline{P}}+\underline{\underline{O}})^{-1} = \underline{\underline{E}}\ [\frac{1}{\lambda+\sigma^2}]\ \underline{\underline{E}}^t \tag{3.5}$$

which again is a diagonal matrix containing the inverted values of the sum of the eigenvalue and the square of the observation error. The analysis equation then becomes

$$\begin{aligned}\underline{a} &= \underline{\underline{P}}^t\ (\underline{\underline{P}}+\underline{\underline{O}})^{-1}\ \underline{d} \\ &= \underline{\underline{E}}\ [\lambda]\ \underline{\underline{E}}^t\ \underline{\underline{E}}\ [\frac{1}{\lambda+\sigma^2}]\ \underline{\underline{E}}^t\ \underline{d} \\ &= \underline{\underline{E}}\ [\frac{\lambda}{\lambda+\sigma^2}]\ \underline{\underline{E}}^t\ \underline{d}\end{aligned} \tag{3.6}$$

The observed data and the analysed values can be projected onto the eigenfunctions $\underline{\underline{E}}$:

$$\underline{d} = \underline{\underline{E}}\ \underline{\delta} \quad ; \quad \underline{a} = \underline{\underline{E}}\ \underline{\alpha}$$

where δ and α are vectors of coefficients, each element representing the coefficient for one eigenvector in $\underline{\underline{E}}$.

$$\underline{a} = \underline{\underline{E}}\ \underline{\alpha} = \underline{\underline{E}}\ [\frac{\lambda}{\lambda+\sigma^2}]\ \underline{\delta} \tag{3.7}$$

or for each eigenvector

$$\alpha_i = \frac{\lambda_i}{\lambda_i+\sigma^2}\ \delta_i \tag{3.8}$$

Thus each mode in the observations is analysed proportionally to the ratio between the eigenvalue and the sum of the eigenvalue and squared observation error. For a fixed observation error (non-zero) the response is stronger the higher the eigenvalue is and modes with low eigenvalues are damped. This is a very instructive way of studying the filtering properties of OI.

A simple example is shown in Fig. 3 for two wind observations (u- and v-components) separated by some horizontal distance r. The correlation model is Gaussian :

$$F(r) = G(r) = \exp(-0.5(\frac{r}{b})^2) \qquad (3.9)$$

where b is a constant length scale. The prediction error correlation matrix is of order 4 and its 4 eigenvectors are shown to the left in Fig. 3. One divergent mode (1), a rotational (2) and two modes representing mean u- and v-winds respectively. At small separations r/b both divergent and rotational modes are efficiently damped (with reasonable values of σ^2, typically around 0.5 in operational analysis schemes). Almost all the weight is on the mean wind. At larger separations between 0.5 and 1.5 the divergent and rotational modes become more important and as ν is increased more emphasis is put on the divergent mode (1) than on the rotational (2). The eigenvalues for mode (1) increase most rapidly for low values of ν although not as markedly as Daley (1985) showed for three wind observations. At large separations these curves become rather meaningless, as pointed out in Daley (1985), since no consideration is given to the analysis at points between the widely separated observation points. The analyses at the two observations points then become largely independent. One might be tempted to paradoxically conclude that a reasonable divergent analysis could be made at separations of say 2 r/b even with ν=0, since the eigenvalue is not much smaller for mode (1) than for mode (2). This is of course only a deception since if the analysis is evaluated on a dense grid one finds two almost separate non-divergent analyses, each just like in Fig. 1a and the divergence zero everywhere. It is just not proper to describe mode (1) as a divergent mode at large distances. The results nevertheless serve to give some insight what to expect from including divergence in OI but it obviously has to be verified in the full 3-dimensional analysis system with a multitude of observations from different sources.

It can be concluded that the exact value of the divergent part of the forecast error (ν) is not crucial as long as it is not close to zero. The value of ν=0.1 gives a ratio of 0.32 between the standard deviation of the divergent part of the wind and the total wind which agrees reasonably well with the results of HL (based on radiosonde winds over North America). Also the effect

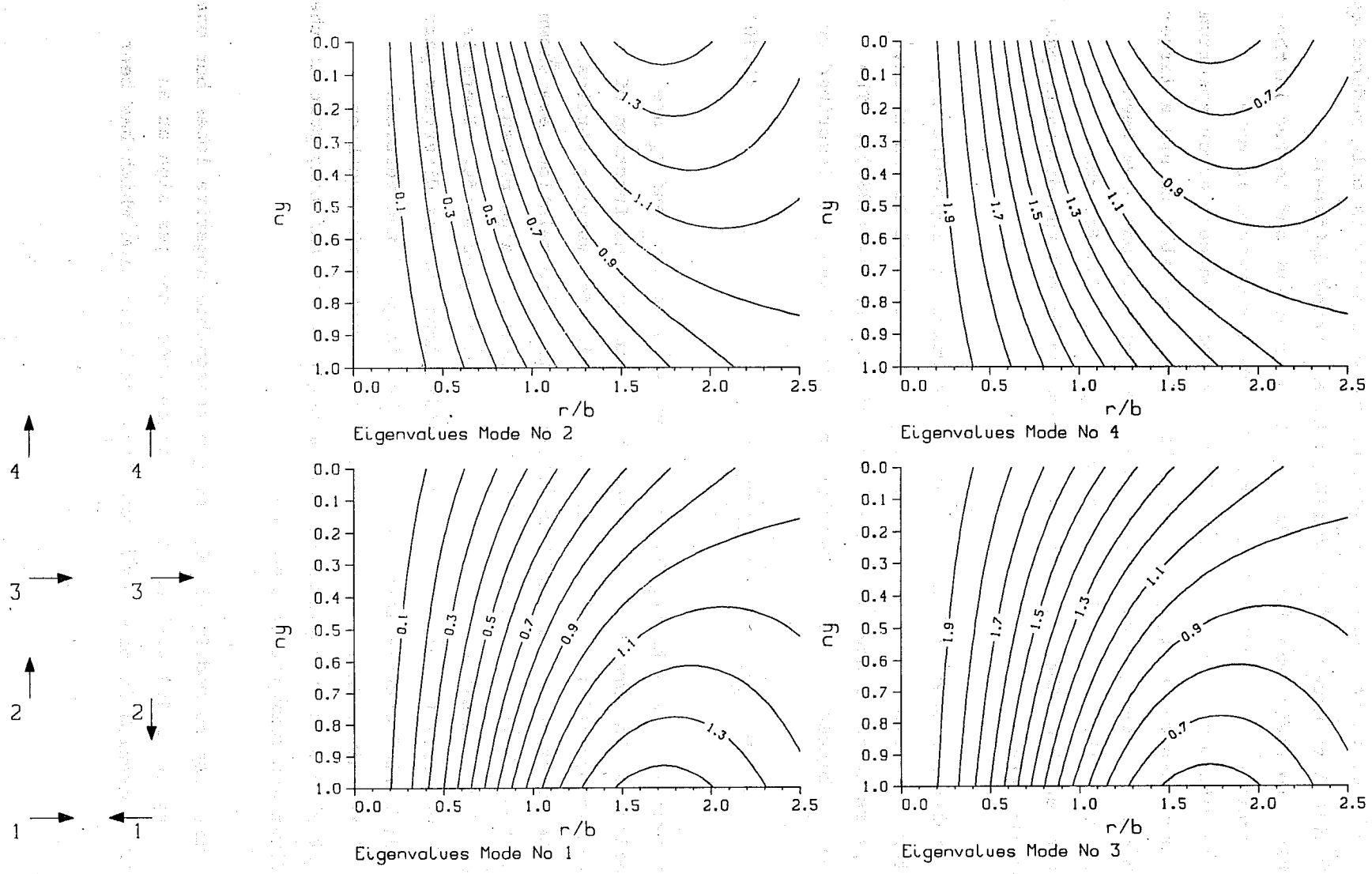

Figure 3. **Eigenvectors and eigenvalues for OI-analysis of 2 wind observations at the observation points. The ordinate is the dimensionless distance r/b and the abscissa the divergent part of the forecast error (ν).**

on the analysed rotational wind should be small with this choice since the standard deviation of the rotational part of the wind error is only reduced by 5%. The vertical structure is indicated in HL and three different approximations to their empirical data have been tried out and tested in the following sections. In the horizontal the divergent structure is more difficult to determine although HL found most of the divergent error spectrum in the large scales and Daley (1983) thought it was desirable to use a larger scale than for the non-divergent one. Therefore two versions have been tested; one using the same scale for the divergent part as for the non-divergent and the other using twice as large scale for the divergent part of the correlations.

The ECMWF analysis system utilizes continuous functions to represent the vertical forecast error correlations enabling data and model levels at any values of pressure to be used (Unden (1984) and Shaw et al. (1987)). The correlation c_{ij} between winds (or heights) at levels i and j is described by

$$c_{ij} = 1\,\frac{1}{e-1}\,\exp\left[\frac{a}{a+(x_i-x_j)^2}\right] - \frac{1}{e-1} \qquad (3.10)$$

where e is exp(1), a is a tuning constant close to 1, and x_i and x_j are transformations of the pressures involved (x is a monotonous function of pressure and is essentially a transformation to allow for varying vertical scales in the atmosphere). Examples of these vertical correlations are shown in Fig. 4. They decrease asymptotically towards zero at large pressure separation which is desirable for heights and non-divergent winds. There is however evidence from HL that there is a negative lobe for the divergent part of the vertical wind correlations. Also from knowledge of the vertical structure of the divergence itself as well as from continuity equation arguments it should be appropriate to have a negative compensating part in the vertical divergent correlation function.

It is not very easy to modify (3.10) and get reasonable negative lobes but one way is to multiply (3.10) with another function which changes sign at an appropriate separation in pressure. The first such function which has been used is

$$1-(6-5a)(x_i-x_j)^2 \qquad (3.11)$$

The constants are chosen so as to get the vertical integral close to zero and the tuning parameter a is used to compensate for the different behaviour of the transformation x in the tropics and extra-tropics (a is about 1.1 in the tropics and just over 1.0 elsewhere). Fig. 4 also shows the resulting correlations when Eq. (3.10) is multiplied with (3.11).

4. ANALYSIS IMPACT OF INCLUDING DIVERGENT STRUCTURE FUNCTIONS

The formulation (3.11) for the divergent part of the correlations and ν=0.1 was used to analyse a case at 861208 00 UTC when observations indicating strong upper level divergence over the western tropical Pacific were poorly analysed operationally at ECMWF. Fig. 5 shows first an analysis with only non-divergent structure functions (ν=0). The map reveals several areas where the analysis departs significantly from the observations. There is a marked southerly outflow at around 7°S extending from 160°E to 180°E. The SATOB's in this area between 160° and 170°E are not drawn to at all. The analysis is drastically improved when the divergent structure functions are included with ν=0.1, as can be seen in Fig. 6. The analysed winds (short arrows) are turned from being easterly to northeasterly and increase in strength, all in much better agreement with the observations. Around the observations of the northerly outflow at around 7°N and between 170° and 180°E the effect is mainly to change the direction of the analysed winds not only in the vicinity of the SATOB's but also some distance away, e.g. along the 180°E longitude all the way down to about 2°S. Here the combined effect of the aforementioned groups of observations seems to be to enhance an east-westerly divergent zone at about 2°S which is hardly present at all in the non-divergent analysis (Fig. 5). Further west, around 4°N, 163°E, the SATOB's indicate quite a bit stronger winds than the non-divergent analysis and including the divergent terms here increases the wind speeds by about 5 m/s towards the observed values. At the equator around 140°E Fig. 5 has a local wind minimum right between two strong SATOB winds. This feature is no longer present in Fig. 6; the analysed winds are increased and turned towards the observed and they vary smoothly in the area. It must be emphasised here that the sole difference between the two analyses displayed in Figs. 4 and 5 is the inclusion of the divergent structure functions for this analysis cycle only. Both analyses use the same first guess.

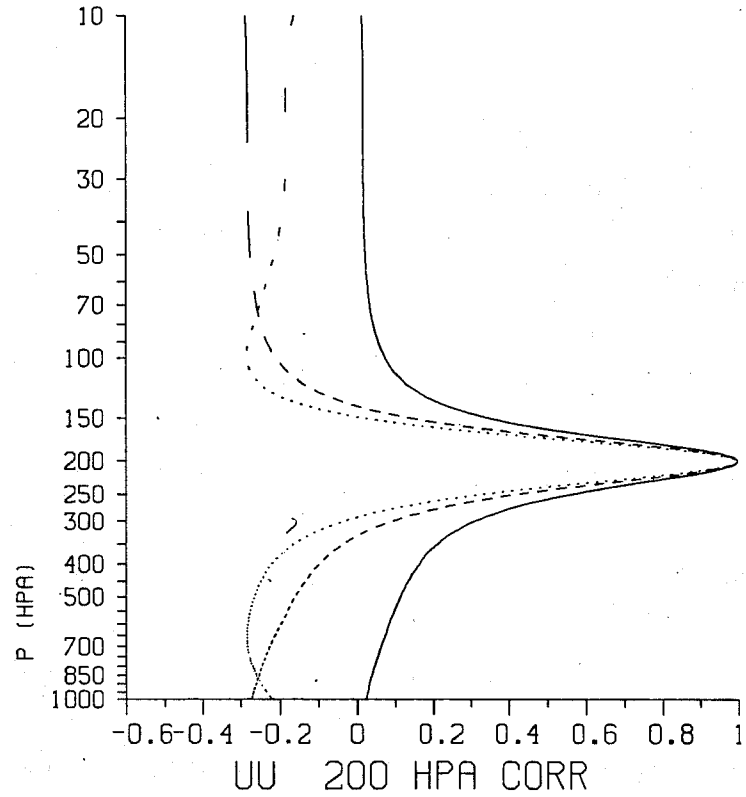

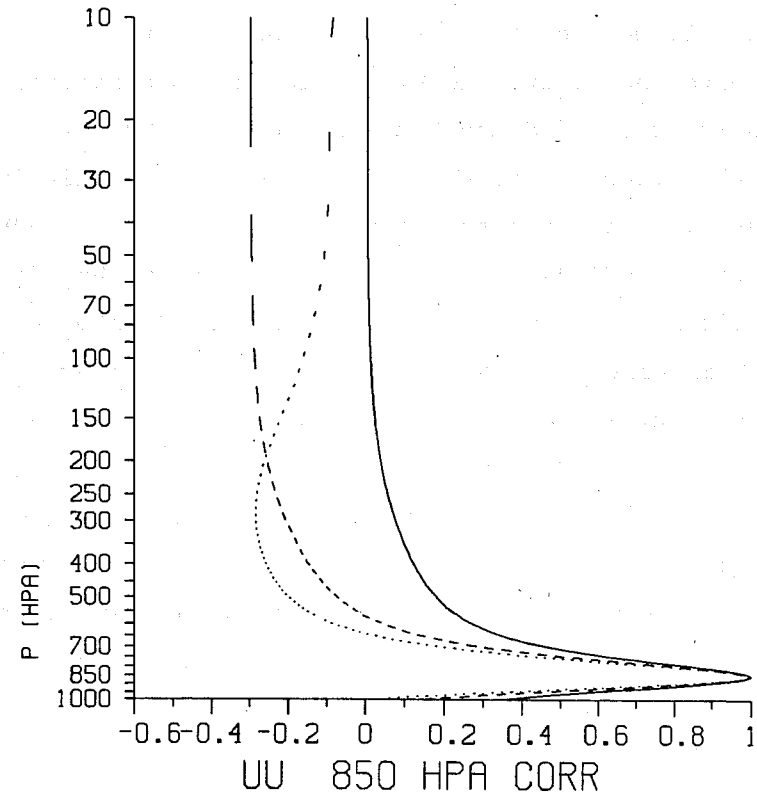

Figure 4. Vertical correlations of forecast error in the tropics between a datum or a gridpoint at 200 hPa and other levels (top) and between 850 hPa and other levels (bottom). Full line is for stream function, dashed curve for the velocity potential using formulation (3.11) and the dotted curve is when formulation (6.1) is used.

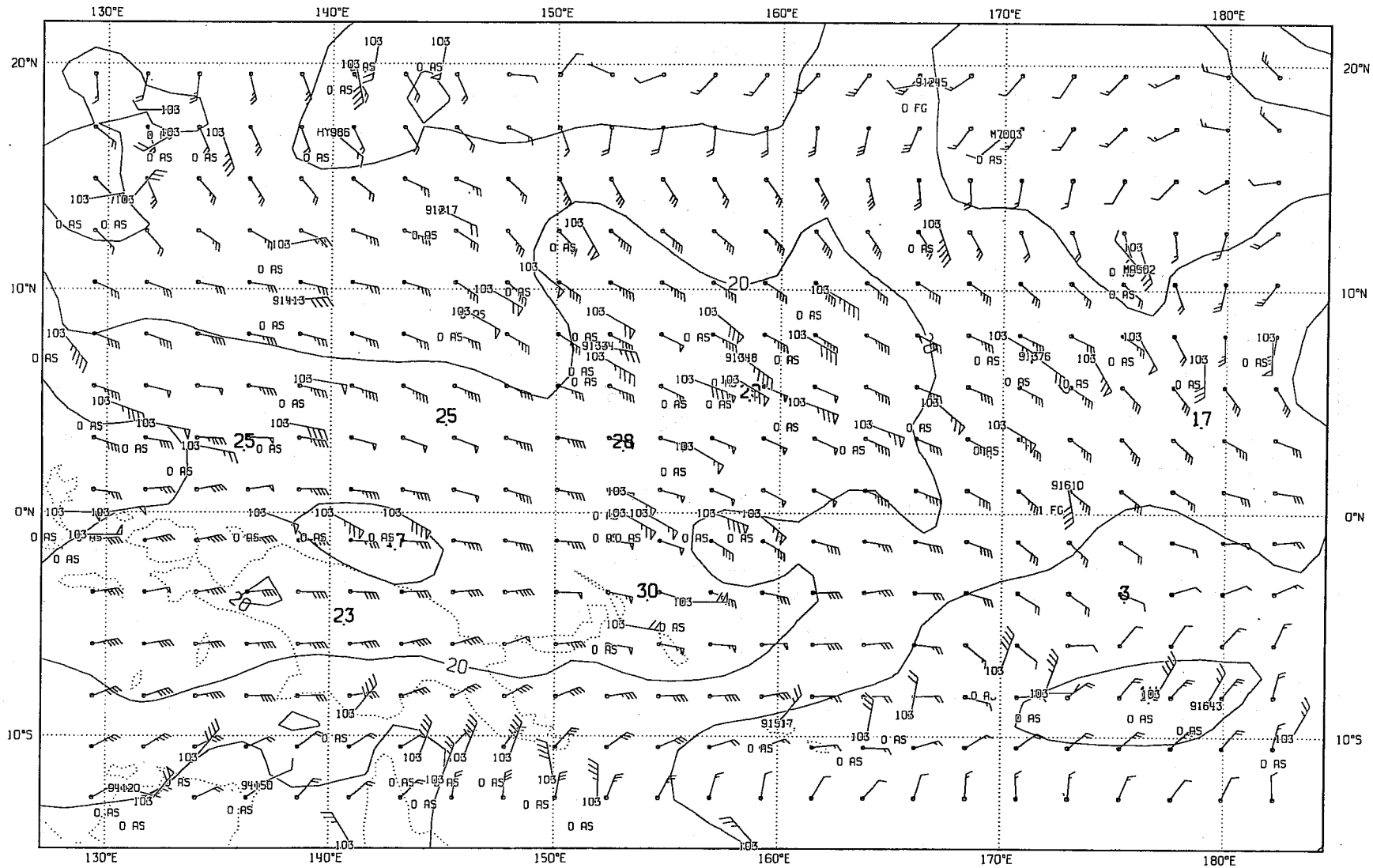

Figure 5. Wind observations and analysis with non-divergent structure functions at 200 hPa 861208 00 UTC. Short wind arrows represent the analysed wind and the isolines are for every 10 m/s.

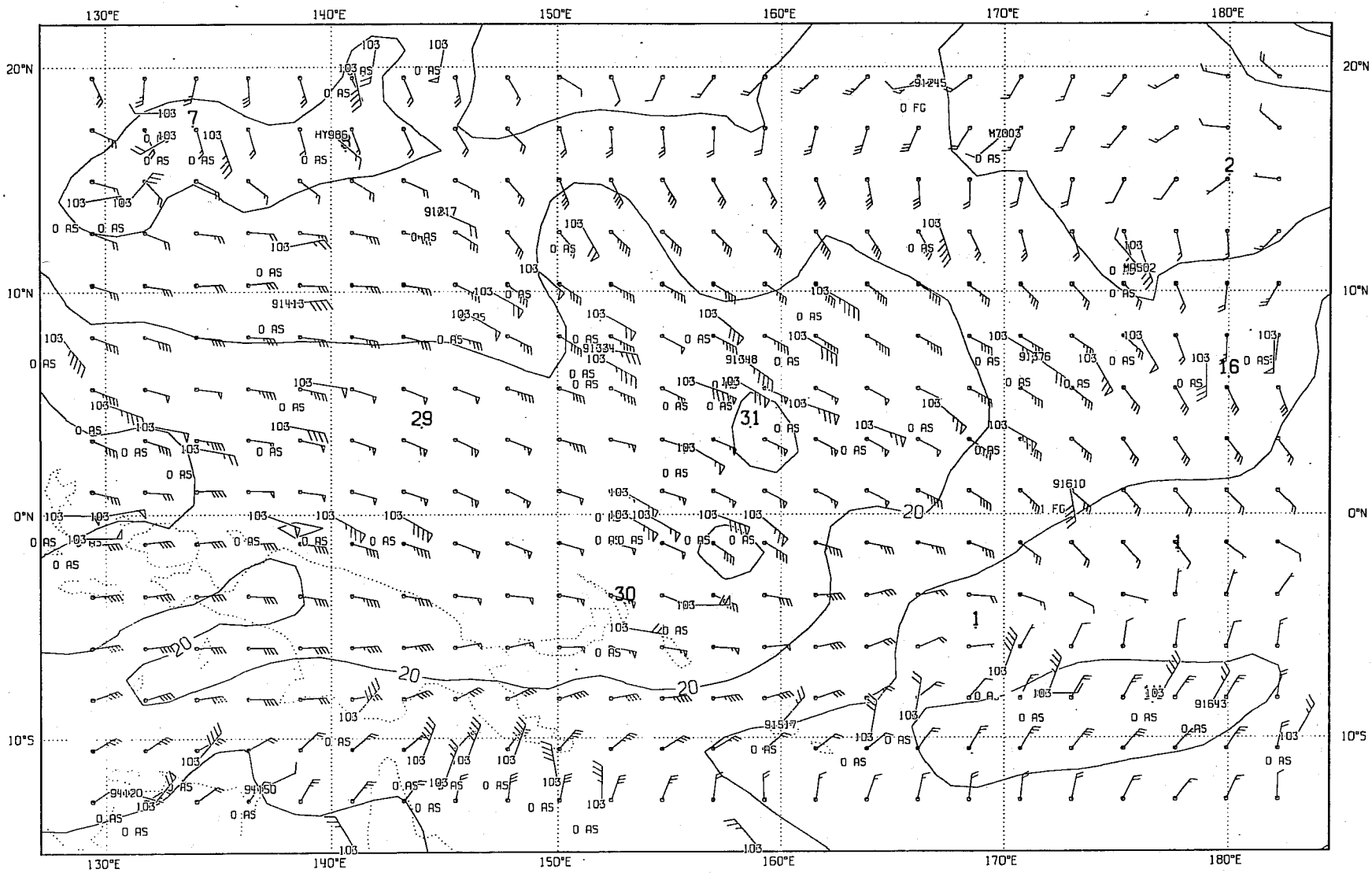

Figure 6. As Fig. 4 but for analysis with divergent structure functions.

A wind difference map (Fig. 7a) over a slightly larger area highlights these features and shows a distinctive divergent signal with magnitudes of up to 10 m/s. Another area where the non-divergent analysis fails completely is at 17°N, 132°E and here the analysis with divergence draws partly to the convective outflow. The horizontal scale of the structure functions is however too large to resolve this relatively small scale feature very well. (In terms of the component length scale Lc, as defined in HL, it is about 800 km at this latitude). This is actually the position of a tropical cyclone (Kim) with observed surface winds of 15-20 m/s and these are rather well analysed even though the analysis did not produce the correct depth (in surface pressure).

The area shown in Fig. 7 includes the highest magnitudes of impact from the use of the divergent structure functions. Elsewhere in the tropics and subtropics the wind impact is smaller and it is generally much smaller in middle latitudes (polewards of 40°N and 40°S).

At other levels the wind impact is reduced in both directions from the 200 hPa level displayed in Fig. 7a. Especially in the boundary layer there are disappointingly small differences; when noticeable at all there are some small areas with differences of only 1-2 m/s at 850 hPa (Fig. 7b) connected with the strong outflows at 200 hPa. Presumably the reason is that there are no low level SATOB winds underneath any of the strong outflow areas mentioned above, which is understandable since extensive high cloud cover would exclude low level observations. The negative lobes of the vertical divergent correlation functions in Fig. 4 may imply some low level divergence (with reversed sign) from upper level winds. This effect is however very small since the 200-850 hPa correlation is about -0.25 and the forecast error standard deviation used in the normalisation decreases by more than 70 % from 200 to 850 hPa. Thus a 10 m/s divergent wind analysis increment at 200 hPa from upper level data only would have at most an -0.75 m/s correspondence at 850 hPa. A small low level impact as in Fig. 7b can be expected unless there are plenty of low level data supporting an inflow structure and this was not the case here.

The sensitivity to variations of the ν-parameter has also been tested for this case. Analyses with ν=0.05 and 0.20 were run and wind differences between these and the non-divergent analysis at 200 hPa are shown in Fig. 8a

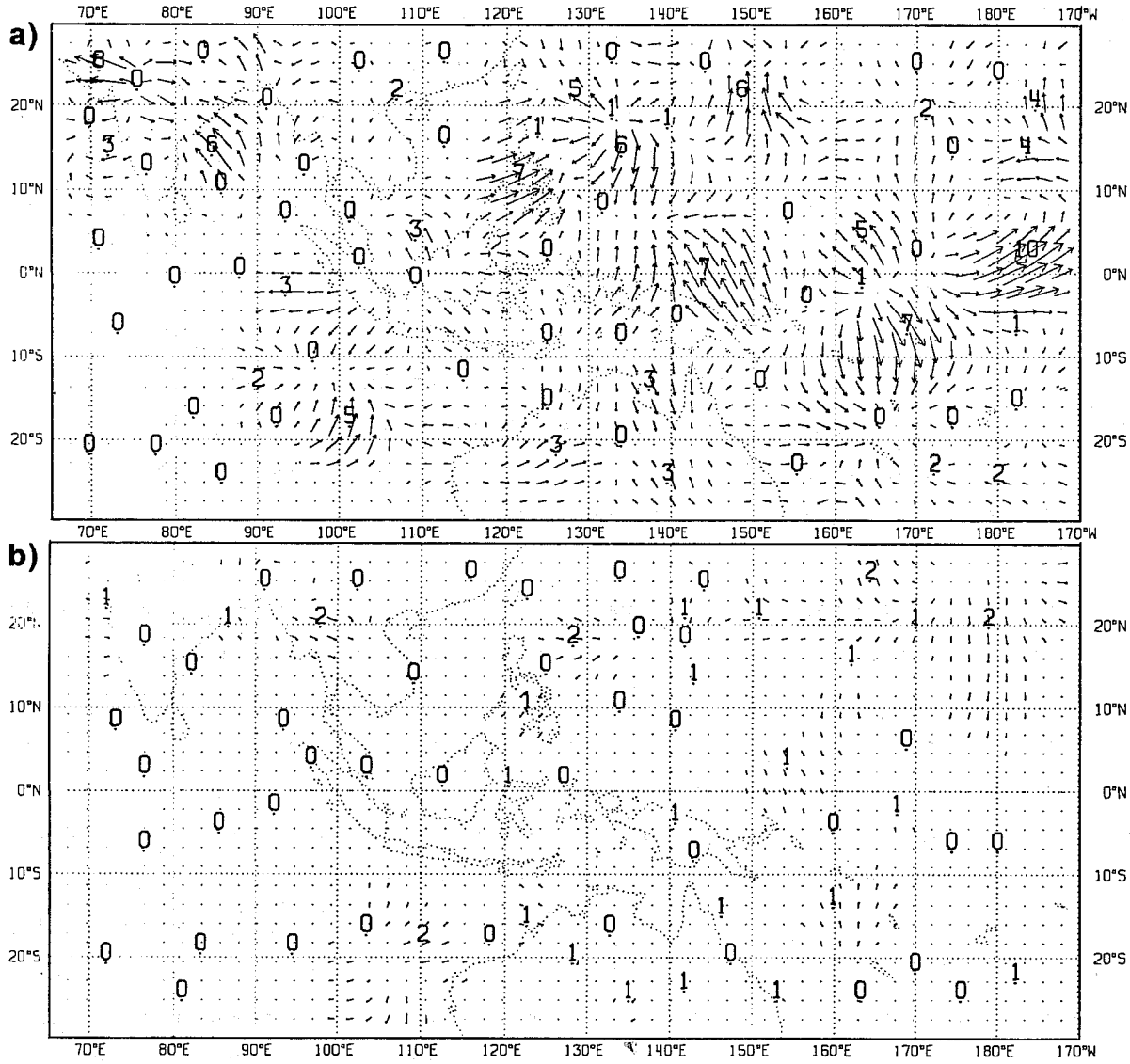

Figure 7. Wind differences 861208 00 UTC between analyses with and without the divergent structure functions at 200 hPa (a,top) and at 850 hPa (b,below). Isoline at 10 m/s and numbers indicate maxima (and minima) in m/s.

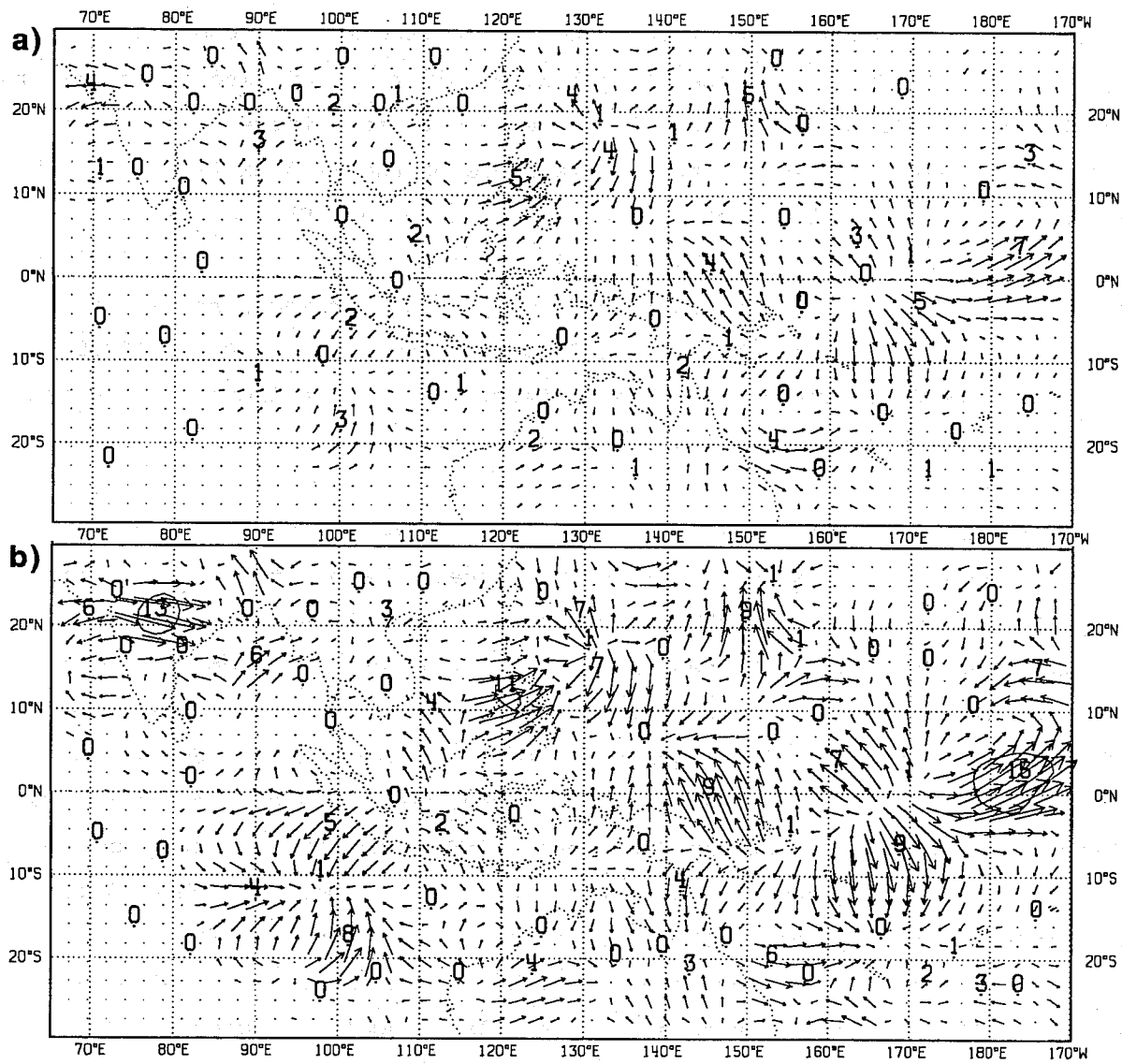

Figure 8. Wind differences 861208 00 UTC between analyses with the divergent structure functions at 200 hPa and with ν=0.05 (a) and ν=0.20 (b). Isoline at 10 m/s and numbers indicate maxima (and minima) in m/s.

and b respectively. These plots should be compared with Fig. 7a, which shows the analysis difference with ν=0.10. It is evident from Fig. 8a that the analysis with ν=0.05 already shows all the divergent features seen in Fig. 7a. Only the magnitudes are somewhat lower. Doubling ν from 0.10 to 0.20 again shows the same structures (Fig. 8b) but the magnitudes are higher than in Fig. 7a. The response is certainly not linear in terms of wind velocities but when the magnitudes of the wind differences are squared there is almost a linear relationship between ν and the variance of the wind differences. The squares of the wind difference maxima (Figs. 7a, 8a and 8b) double as ν is doubled from 0.05 to 0.10 and 0.20. This might have been anticipated since the definition of ν (2.3b) is in term of wind error variance, not standard deviation. In fact, also the results from the case study in Daley (1985) indicate a steady increase in analysed divergence as ν is increased and they do not conflict with the results described here.

To further highlight the impact of using the divergent formulation the analysis increments (analysis field - first guess field) of divergence are shown in Fig. 9; first with the non-divergent correlations (Fig. 9a) and then with the divergent part included (Fig. 9b). It is evident from Fig. 9a that there is already a significant divergence in the non-divergent case through different data selection in neighbouring boxes as explained in Section 1. This method of introducing divergence is rather noisy ; e.g. the large area of divergent increments between 140°E and 170°W is interrupted here and there by spots of no divergence. Such features disappear completely when allowing explicitly for divergence in the OI-equations as seen in Fig. 9b. The field has now a nice and smooth appearance. Although many features existed already in Fig. 9a they are now continuous and have large scale structures. Any fears of a detrimental effect on the vorticity analysis can be allayed by comparing the analysis increments of vorticity from the two analyses in Fig. 10a and b. This field is virtually unchanged by the modification as was suggested earlier in Section 3.

The analysis increments of divergence for the other analyses (with ν= 0.05, and 0.20) are shown in Fig. 11. They show that the squared divergence increments increase somewhat less than linearly with ν (also compare Fig. 9 b). The wind differences shown earlier (Figs. 7a and 8) were in fact not

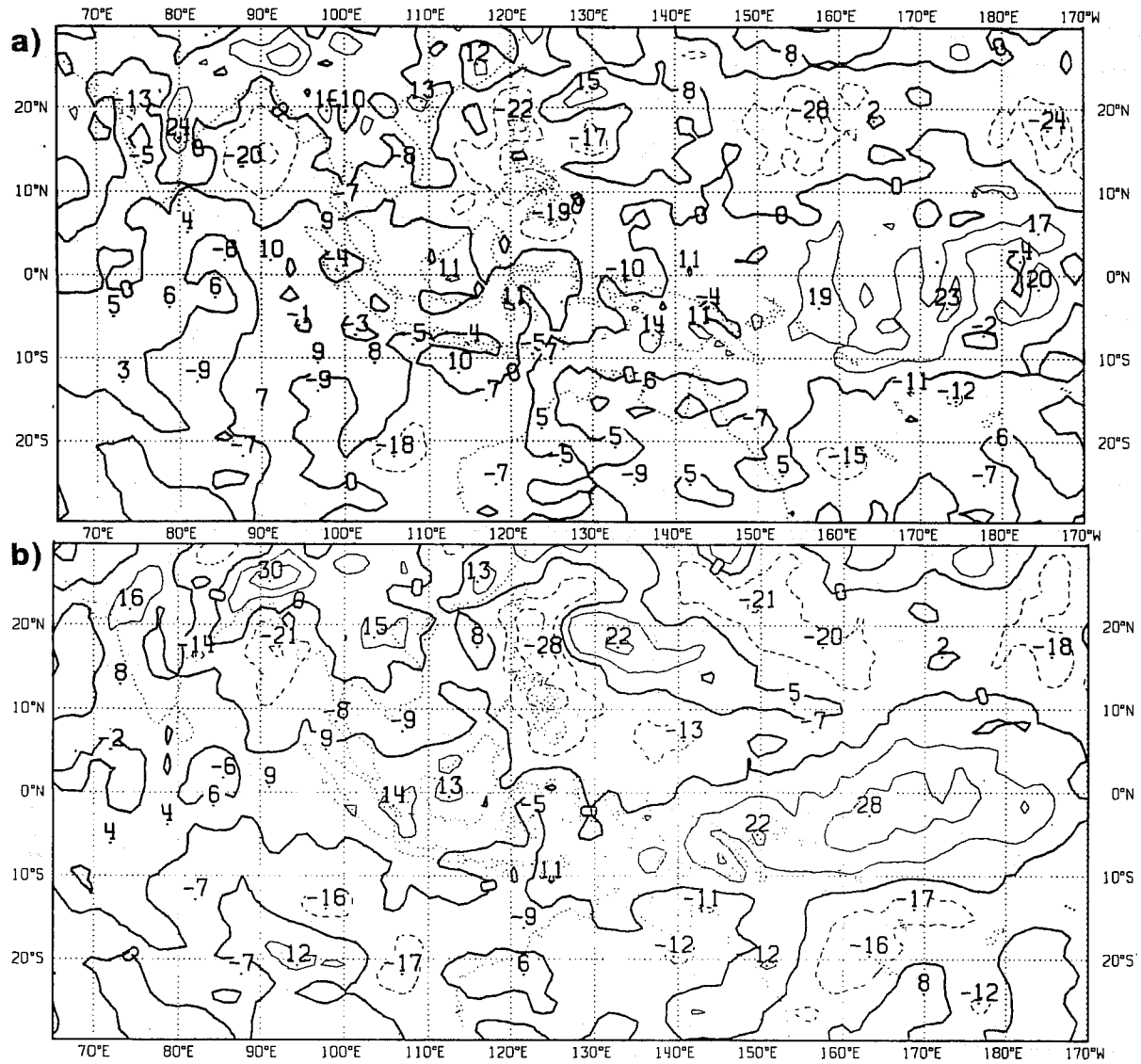

Figure 9. Analysis increments of divergence at 200 hPa 861208 00 UTC when analysing with the non-divergent structure functions (a,top) and the divergent ones (b,below). Unit is 10^{-6} s^{-1} and isolines are for every 10^{-5} s^{-1}.

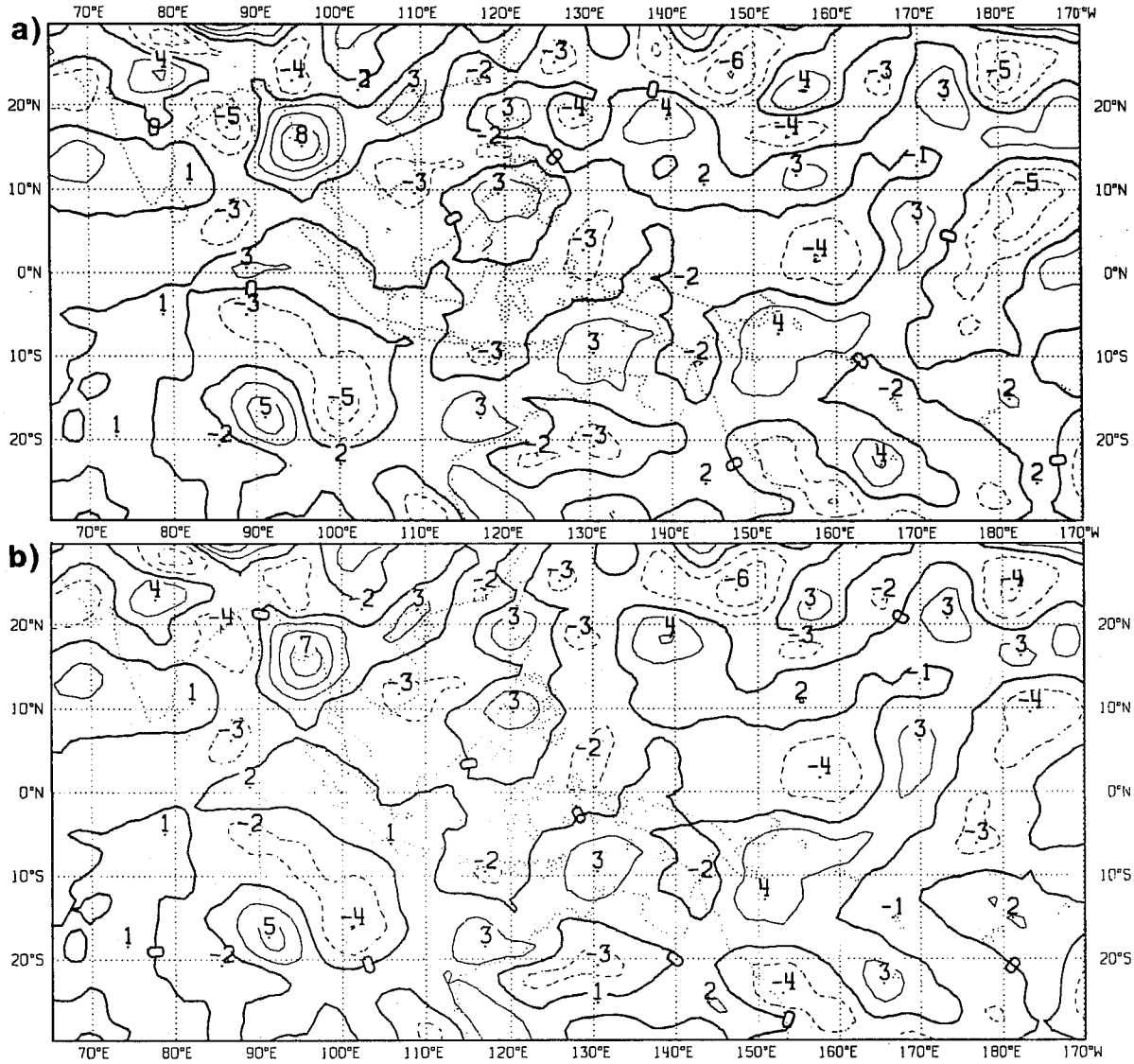

Figure 10. As Fig. 7 but for vorticity. Unit is 10^{-5} s^{-1} and isolines are for every $2*10^{-5}$ s^{-1}.

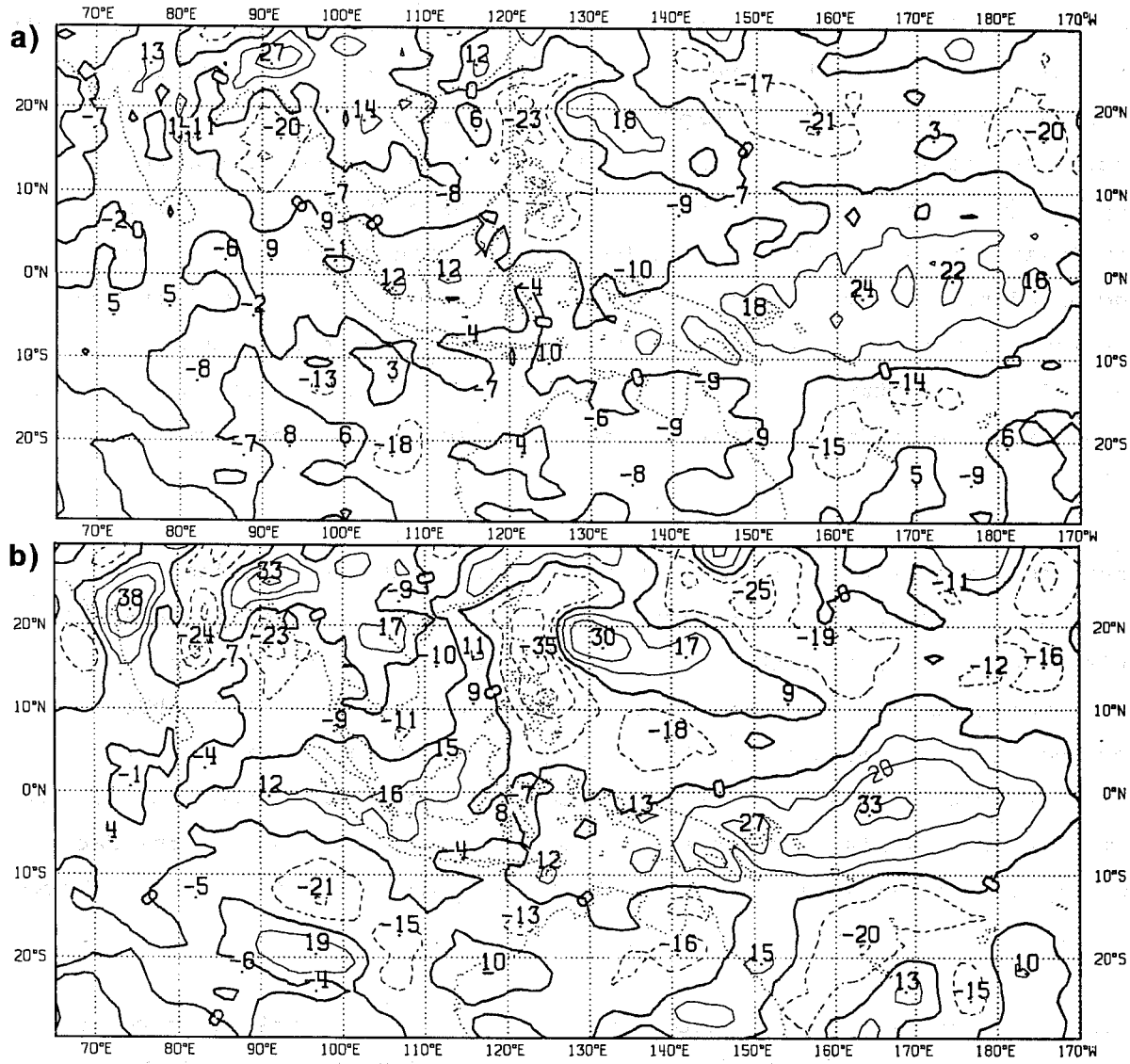

Figure 11. Analysis increments of divergence at 200 hPa 861208 00 UTC with the divergent structure functions at 200 hPa with ν=0.05 (a) and ν=0.20 (b). Unit is 10^{-6} s^{-1} and isolines are for every 10^{-5} s^{-1}.

completely divergent and thus the response in terms of variance of divergence is slightly less than linear in ν.

There is also an additional wind difference over northern India in Fig. 8b which is not directly related to the divergent structure functions. It is due to an acceptance of a TEMP wind which is rejected in all the other analyses with lower values of ν. This might be due to the change in wind correlation patterns but could also be a result of less of a geostrophic coupling in OI-system (Eq. 2.8) when ν is increased. This also affects the estimated OI-analysis errors and they tend to be slightly larger when the divergent structure functions are included. This has a consequence for quality control since the estimated interpolation errors are used to normalise the observational departures. This normalised value may then be reduced to fall within one of the data rejection limits (see also Hollingsworth et al. (1986)).

Another question is whether the normal mode initialisation retains the divergence introduced by the modification. Comparing the two analyses after initialisation shows that the major part of the analysis differences (from Fig. 7) remain as Fig. 12 shows. In the major outfow areas at 200 hPa described earlier almost all of the divergent wind impact is retained. Judging from other areas and levels it seems that on average about 2/3 of the original wind analysis difference remains. This probably owes to the fact that only 5 vertical modes in the ECMWF 19-level model are initialised (Wergen (1987)).

The improved analysis of wind data noted earlier is systematic in terms of root mean square (RMS) differences between observed TEMP winds and the analysed ones as Fig. 13 shows. The improvement is also carried through in terms of fits to the initialised fields in the troposphere but to a lesser degree than what might be inferred from the initialised horizontal differences (Fig. 12). In the extra-tropics (outside +/- 20 degrees) there are also improved fits to TEMP's as well as to PILOT's although less marked than in the tropics.

To summarize, it has been shown that the introduction of the divergent part of the wind-wind correlations gives an immediate and rather strong response in

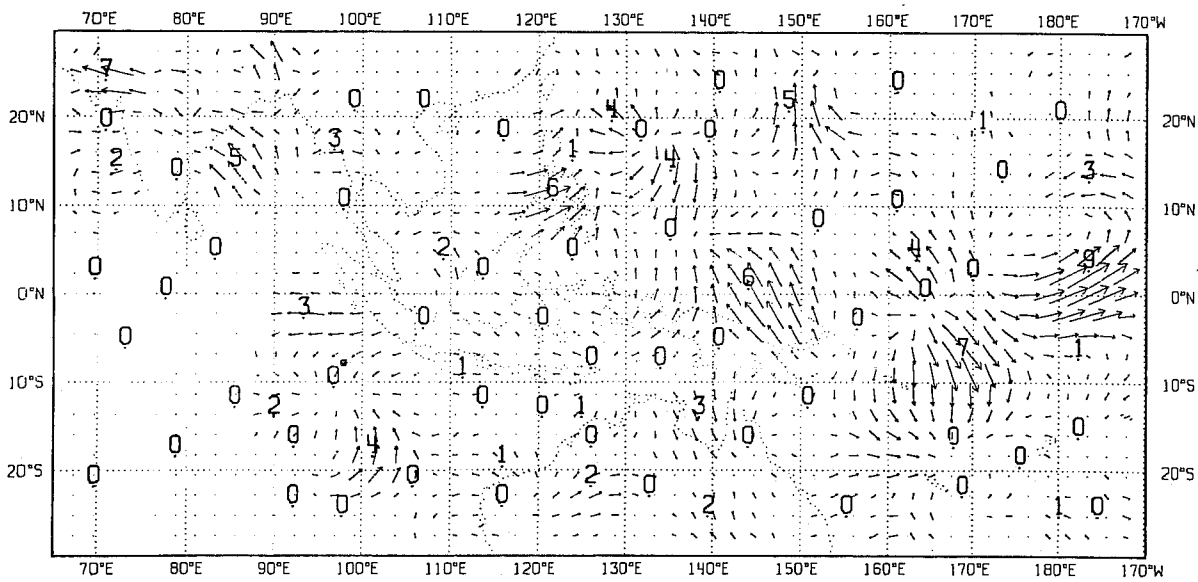

Figure 12. Wind differences at 200 hPa 861208 00 UTC between initialised analysis with divergent structure functions and the initialised analysis with the non-divergent ones. Isoline at 10 m/s and numbers indicate maxima (and minima) in m/s.

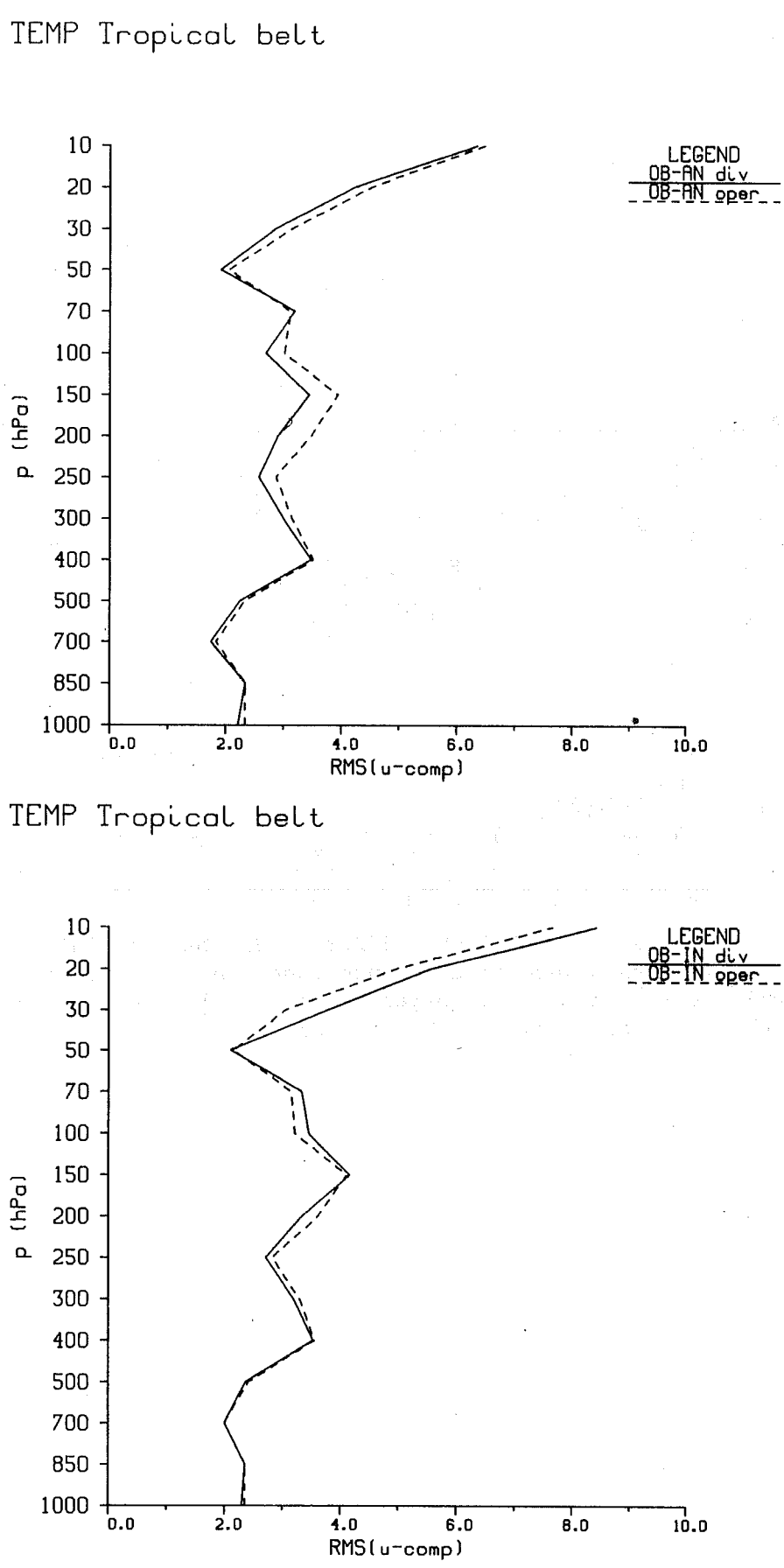

Figure 13. RMS-fits of TEMP u-component winds at 861208 00 UTC in the tropics (20°N - 20°S) to the analysed (top) and initialised fields (below). Full line is with divergence in the structure functions and dashed line without.

the analysis of divergent wind data. It makes the analysis draw much closer to such data and the wind field appears more realistic. There is no evidence of increased level of noise. On the contrary including the divergent terms in the analysis gets rid of the noise caused by the non-divergent constraint whilst hardly affecting the vorticity. The overall effect on the wind field is thus an improvement both in terms of fit to the data and smoothness of the field and perceptibly a more realistic analysis.

5. TESTS IN DATA ASSIMILATIONS AND FORECASTS

The period 861206 00 UTC to 861208 12 UTC was chosen for testing the divergent formulation (3.11) in a data assimilation cycle. This period includes the situation investigated in previous section. One of the points of interest here is to see whether the improvements of the divergent increments can be preserved to some degree, not only after initialisation but also in the first guess forecast which is used for the next analysis in the assimilation cycle.

Throughout this assimilation analysis and initialisation fits to wind data were improved in just the same way as described in the previous section. During the period there were often cases of divergent impact on the analyses similar to those noted before. Wind differences between the test and operational analyses have been studied in detail, mainly in the tropics and subtropics where they were largest. The impacts did survive the initialisation to a large degree but were significantly damped during the ensuing 6 hour forecast. They were then dispersed either in the next analysis or the next first guess forecast. Height differences were insignificant except sometimes locally in case of a datum being rejected in one analysis and not the other.

It is worthwhile to study the situation of 861208 00 UTC again and compare with the single analysis in previous section. The impact on the wind analysis of including the divergence in the structure functions can be seen in Fig. 14 and should be compared with Fig. 7a which is valid for the same time. The differences now are that the experimental analysis has been preceded by two days of data assimilation (8 6-hour cycles) and that the operational analysis, which is the reference in the comparison in Fig. 14, did not have the extra smoothing achieved by the improved analysis box averaging technique since introduced operationally. All the major details from the one cycle analysis

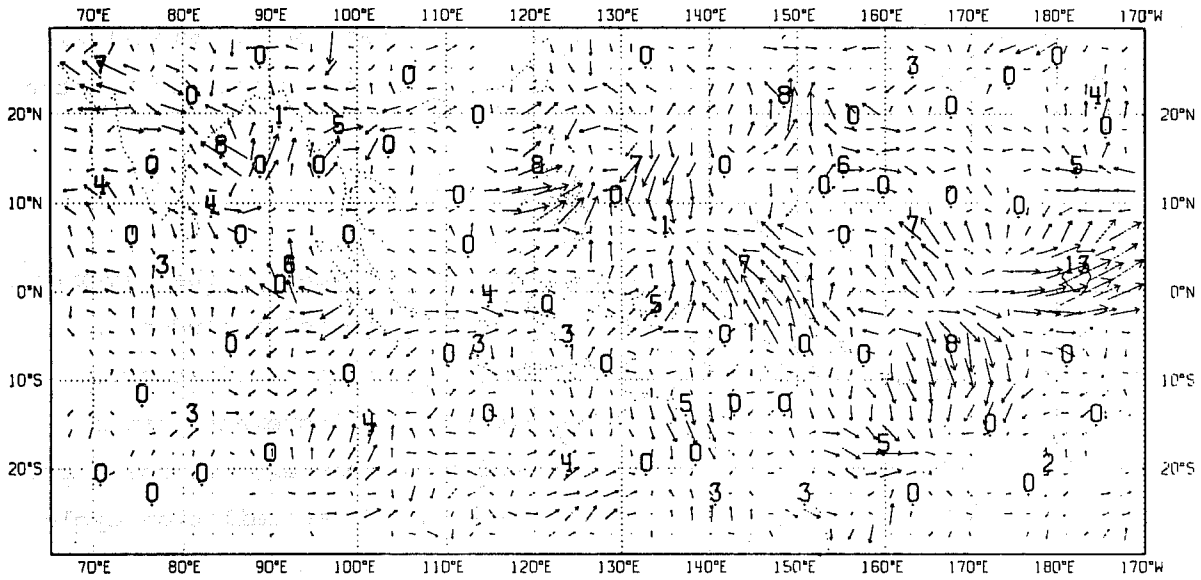

Figure 14. Wind differences at 200 hPa 861208 00 UTC between the analysis from the assimilation including divergence and the operational analysis. Isoline at 10 m/s and numbers indicate maxima (and minima) in m/s.

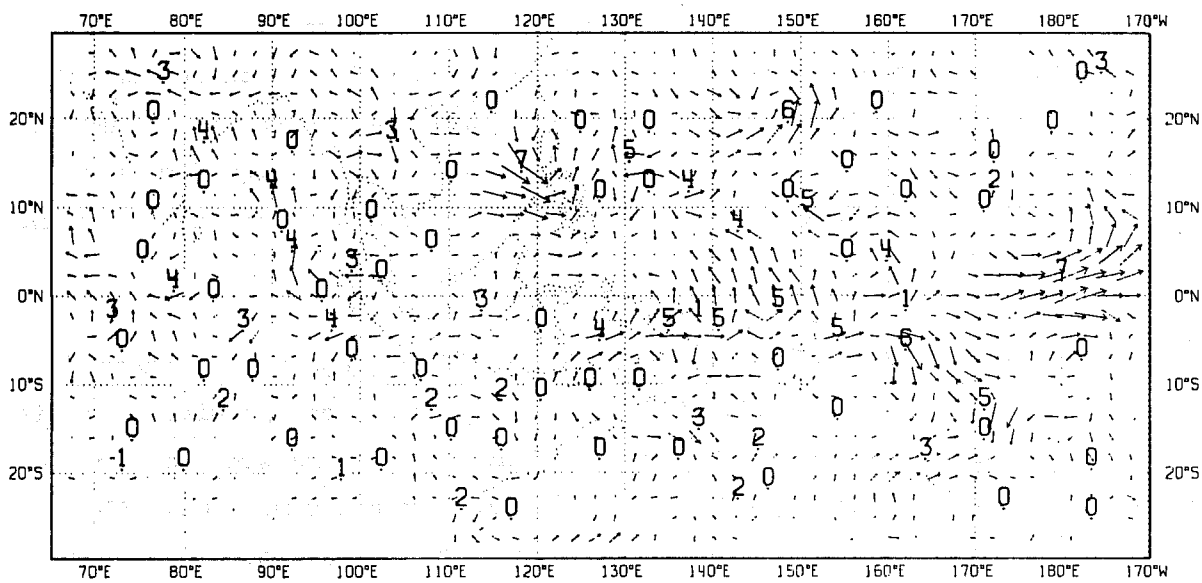

Figure 15. As Fig. 11 but between the ensuing first guess forecasts at 861208 06 UTC.

in Section 3 are still present with the same or slightly higher magnitude. Also small scale features appear as a result of the preceding assimilation with divergence included. The initialisation still retains a large part of the impact. When comparing the test assimilation 6 hour first guess forecast for 06 UTC with the operational first guess (Fig. 15) there is a significant damping of the magnitudes but still over half remains. This may seem relatively satisfactory but these sorts of signals is usually annihilated in the ensuing analysis if data present or otherwise in the next 6-hour forecast step.

This assimilation was repeated with another choice of vertical correlations for the divergent part of the wind forecast error, namely the one with the same vertical formulation as for the non-divergent part and thus without negative lobes (see also Fig. 4). The only significant differences between the analyses are the expected ones, namely that the divergent impact becomes more spread in the vertical when the negative lobes are not utilized. The divergent impact from data at 200 hPa is slightly increased at e.g. the 300 hPa and 100 hPa levels and beyond. The impact at low levels implied by high level winds is absent in the assimilation which doesn't use negative lobes but this effect is rather small anyway.

The RMS-fits to wind observations are very similar as well, although some minute advantage can sometimes be discerned in favour of the assimilation with the negative lobes.

Some impact on the convective precipitation in the 6-hour forecasts might have been expected but the results are disappointing. Both assimilations display very similar fields and they are both rather similar to operations too. The patterns are the same, only the maxima vary slightly.

10-day forecasts were run from 861207 and 861208 12 UTC from both assimilations. Extra-tropical (20-82.5 degrees of latitude) height anomaly correlation scores for the forecasts from 861208 are displayed in Fig. 16 for the two tests. The impacts in terms of anomaly correlations are small for both hemispheres when compared with the then operational forecast based on non-divergent analyses. Out of the two test forecasts the second one based on analyses with negative lobes (F40 in Fig. 16) seems to have a slight edge over

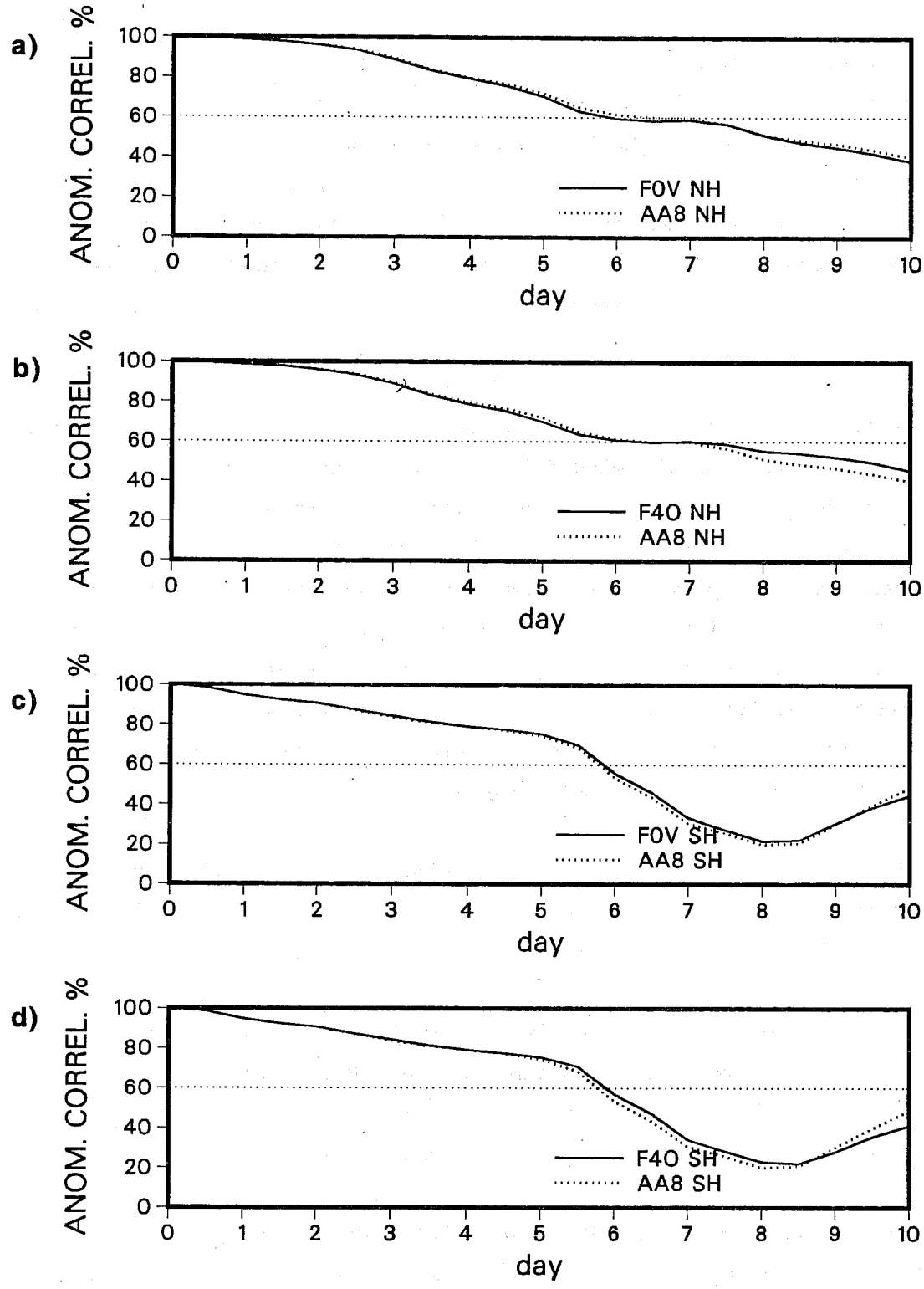

Figure 16. Height anomaly correlations averaged between 1000-200 hPa in northern hemisphere extra-tropics for forecast from 861208 12 UTC based on the assimilation using divergent structure functions with the same vertical fomulation as for the non-divergent ones (a) at the top and for the forecast at the same time from the assimilation with negative lobes (b). The dotted line shows the corresponding operational forecast scores. Then the southern hemisphere scores are shown below in (c) and (d) for the same forecasts based on the same vertical formulation and negative lobes respectively.

the one from the assimilation without negative lobes for the divergent structure functions.

With the forecast results in hand it seems justified to use a formulation which has negative lobes for the vertical correlation of velocity potential. This is also in agreement with HL as well as with the conceptual model of high level outflow coupled with low level inflow for large convective systems in the tropics, assuming that the first guess forecast for these structures is poor.

6. FURTHER TESTS IN ASSIMILATIONS OF A SECOND PERIOD

The next period selected for testing was from 870822 12 UTC for five days until 870827 12 UTC. The previously selected formulation for the velocity potential forecast error (3.11) was used in the first assimilation of this period. Also another improved formulation was tried out in a re-assimilation of the same period. The expression used to multiply the non-divergent vertical correlation (3.10) is now

$$(1-.75(x_i-x_j)^2)/(1+.04(x_i-x_j)^2) \qquad (6.1)$$

This expression gives an improved shape of the negative lobes so as to limit the vertical extent of the negative part a little and as to have an asymptotic return to zero for large pressure separations. Although not reproducing the curves in HL with any accuracy this formula gives a more appealing structure as shown in Fig. 4. The re-assimilation with this formulation was extended for a further two days to 870829 12 UTC.

Throughout the assimilations many cases with distinct divergent impacts like the one described in previous sections can be found. The area with most distinct signatures is still the western tropical Pacific and at 00 UTC. The divergent upper level outflow is described mainly by SATOB observations just as before and the test analyses draw much more faithfully to them than the operational ones. Also a different type of impact was noted here and it is the reduction of the return flow implied by the cross-correlations between the wind components. This well known feature of non-divergent structure functions appears in the negative areas of the wind correlations in Fig. 1 and the analysed flow implied by one wind observation is reversed in that area. It is

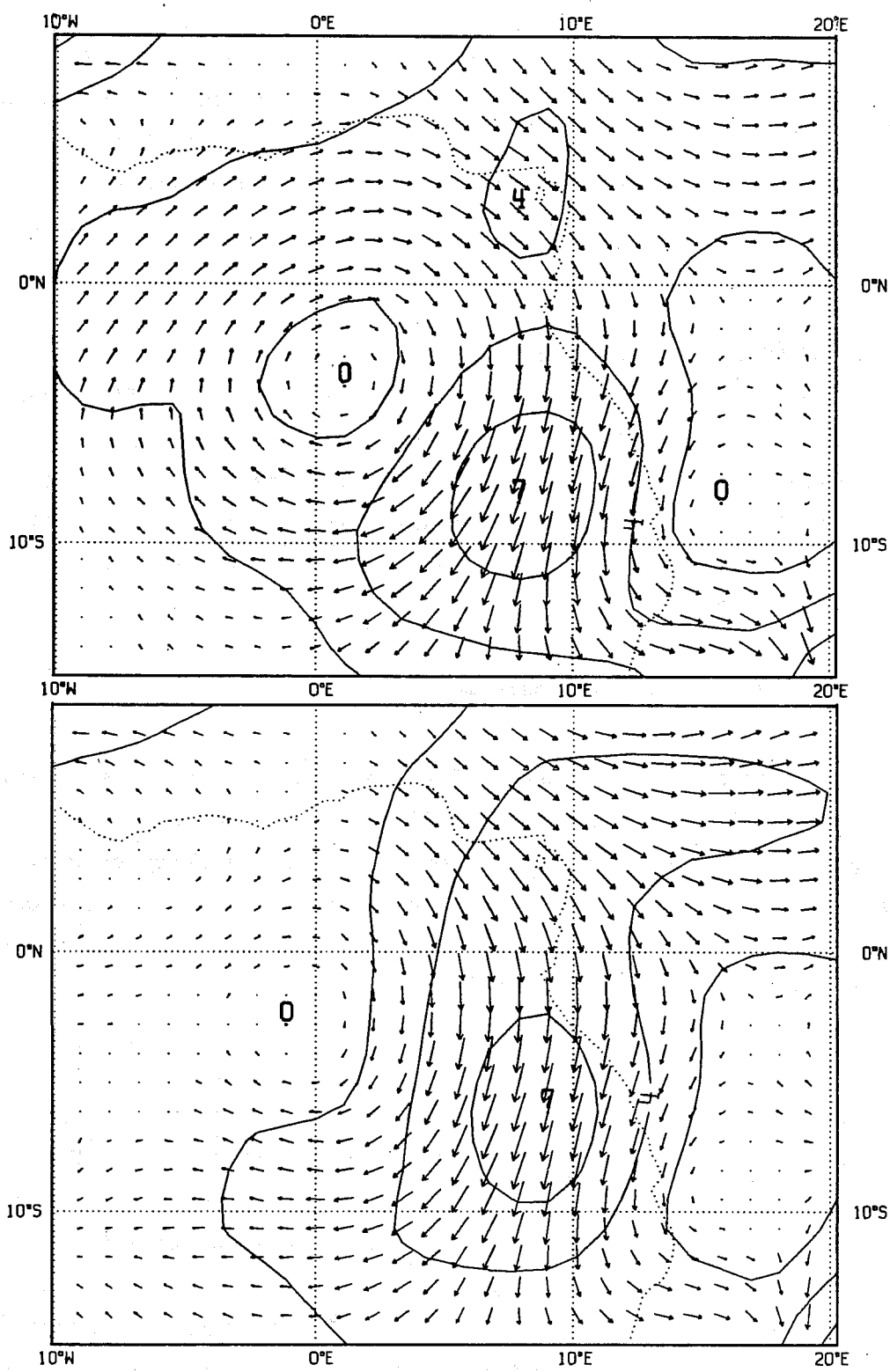

Figure 17. Wind analysis increments at 200 hPa 870823 00 UTC for operations at the top and from the assimilation using divergent structure functions (vertical formulation (3.11)) at the bottom. Isolines are for every 2 m/s.

a natural consequence of imposing non-divergence and enforcing a closed rotational circulation. The most striking example found of this effect is shown in Fig. 17 for 200 hPa off the Central African coast. SATOB observations around 10 E at 200 and 250 hPa have caused a northerly wind increment there and the operational analysis has a distinct southerly return flow at around 5 W as well as a westerly one just north of the equator. Introduction of the divergent terms seem to reduce this impact of the non-divergent structure functions rather well as Fig. 17b shows. This effect is often found when examining the analysis increments from the tests although usually not as strong as the one shown here.

The RMS-fits to wind data (TEMP,PILOT,SATOB and AIREP) are improved also in these assimilations. This is most pronounced for the fit to the analysis fields although some improvement also remains after initialisation. The fits of the first guess forecasts are not discernibly improved. There is no preference in terms of fits to the data for either of the vertical formulations tested here and only results for the latter one (6.1) is displayed here. Fig. 18 shows composite RMS-fits of TEMP u-component winds to analyses and initialised fields in the tropics for this assimilation compared with operations at 12 UTC over the 5 days (containing 6 12 UTC analyses). There is a significant improvement of the analysis fit throughout the atmosphere and which is present for all cycles during the assimilation. The impact on the initialised fields is smaller but is positive everywhere except at the highest few levels. This deterioration is much more limited than the one indicated in Fig. 13 for the one cycle analysis and there is no real cause for concern. Moreover the number of data decreases very rapidly with height in the stratosphere and the sample becomes too small in the tropics. In the troposphere there were more than 300 TEMP wind data for these 6 12 UTC analyses, in the stratosphere less than 200 and only 110 and 43 at 20 and 10 hPa respectively. When it comes to the fit to first guess fields there is no difference between the test and operations. The curves for the v-component of the wind are very similar to the ones for the u-component. In the southern hemisphere the impact is just as strong as in the tropics but in the northern hemisphere the impact is less pronounced.

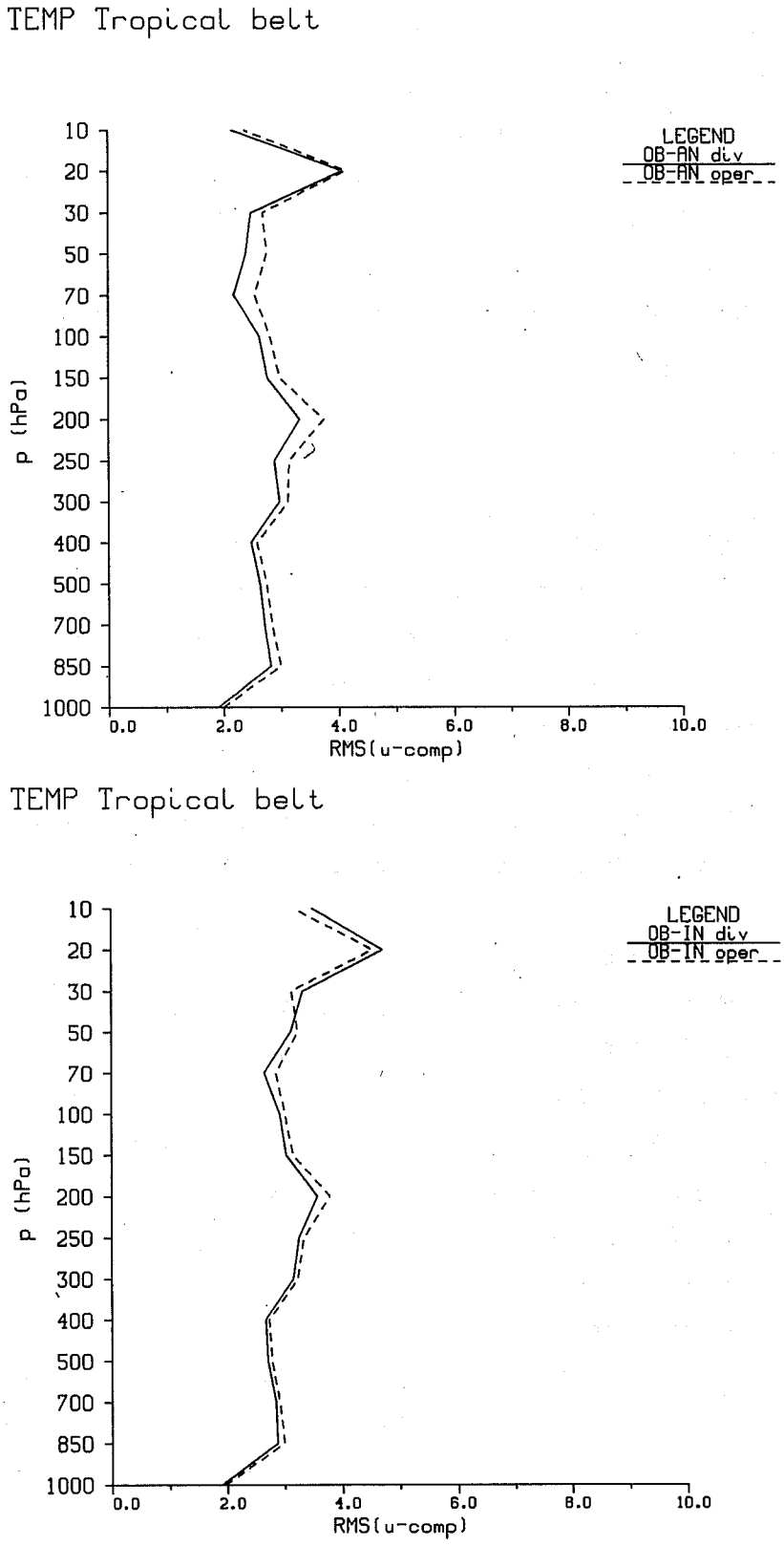

Figure 18. Composite RMS fits of TEMP u-component winds in the tropics to analysed (top) and initialised u-components (below) for 12 UTC from 870822 to 870827 inclusive. Full line is from the assimilation with divergent structure functions using formulation (6.1) and the dashed line is from the operational assimilation with non-divergent structure functions.

Data rejections during these tests were very similar to the operational ones, although occasionally one or two AIREP, PILOT or TEMP winds less were rejected in the tests.

Forecasts were run from both assimilations for 870823 and 24 12 UTC; the scores showed a slight improvement around the 60% anomaly correlation level for one case and a slight deterioration for the other. There was however little to choose between one or the other of the two assimilations. A further five forecasts were run from the second assimilation and average scores are displayed in Fig. 19 for both hemispheres and are compared with operations. The northern hemisphere scores are very similar to operations till around day 5 and the 60% level from which there is a slight deterioration in the test forecasts but they are confined to correlations around 60% and below. The individual forecasts also showed sensitivities in this range (positive and negative) but they were small. Even though the test done here do not indicate any clear difference between the two vertical formulations of the negative lobes ((3.11) and (6.1)) the latter one is conceptually more attractive and was selected for more extensive testing through additional 10-day forecasts whose scores were shown in Fig. 19. This formulation with ν=0.1 and the horizontal scale the same for both stream function and velocity potential forecast error has been implemented operationally 880126 at ECMWF.

Finally the first two days of this period were also assimilated with divergent structure functions using a twice as large horizontal length scale in order to analyse the larger scales of the divergence as suggested by Daley(1983). The effect on the analyses was to significantly reduce the impact seen in all previous experiments. The data indicating strong divergence are much less drawn to and the RMS-fits are less improved than before. Analysis increments of divergence now partly suffers from the noisier behaviour of the non-divergent analysis displayed in section 3 as is demonstrated in Fig. 20. This assimilation does not adequately draw to the divergence and is a rather poor half measure between the non-divergent and divergent systems tested earlier. Also the two forecasts run from this assimilation showed some slight detrimental effect although the impact is slight. This might be expected since it is a test of a modification which is essentially a half measure.

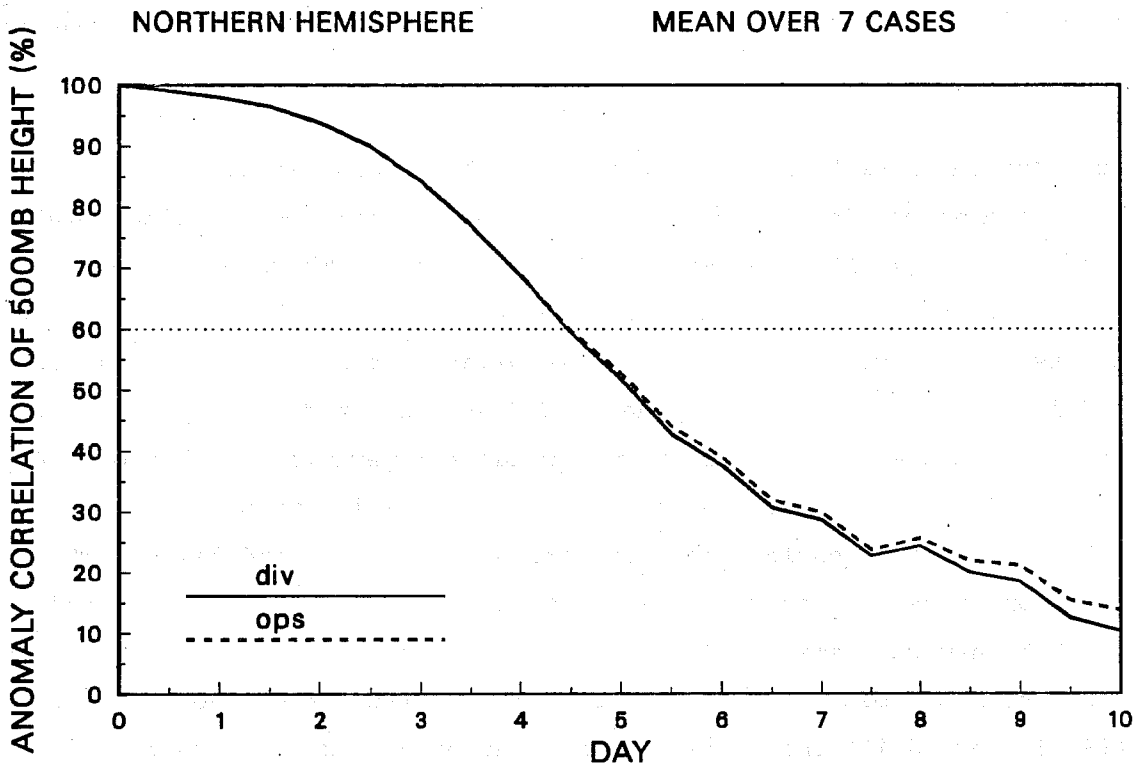

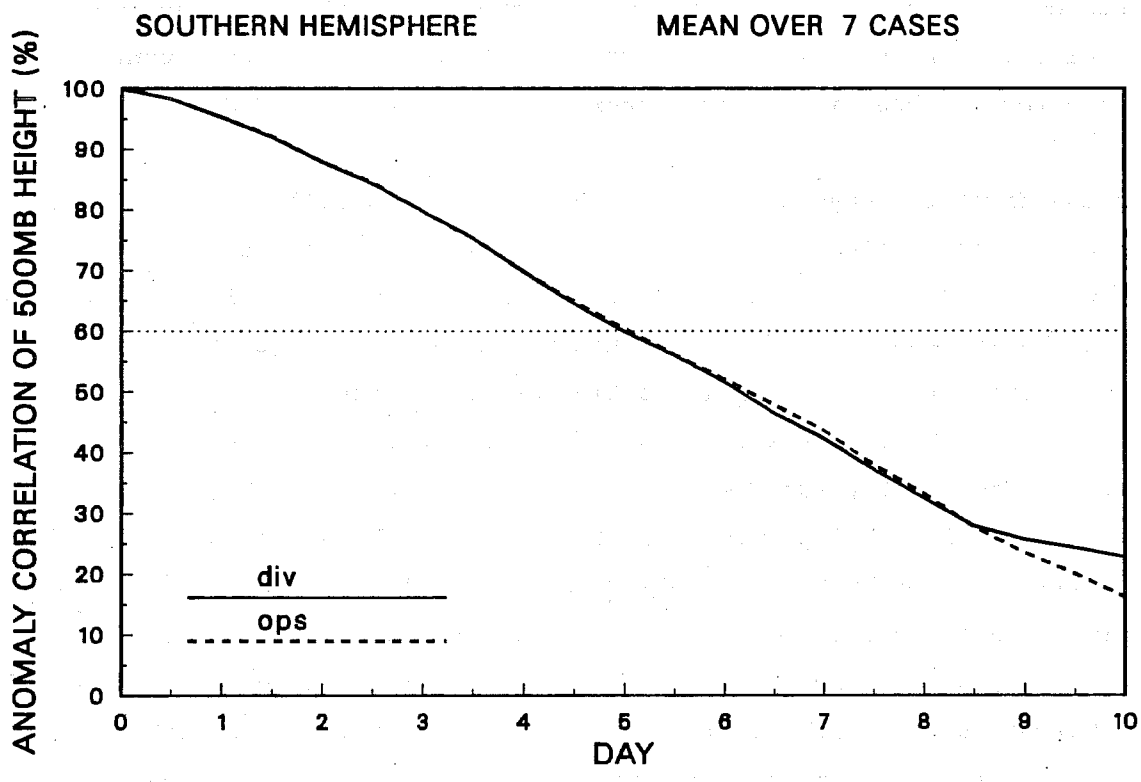

Figure 19. Averaged forecast height anomaly correlations for forecasts from the assimilation using the vertical formulation (6.1) (full line) and operations (dashed line). The initial dates are 870823 to 870829 12 UTC inclusive and the top diagram is for the northern hemisphere extra tropics and the bottom one for the southern hemisphere.

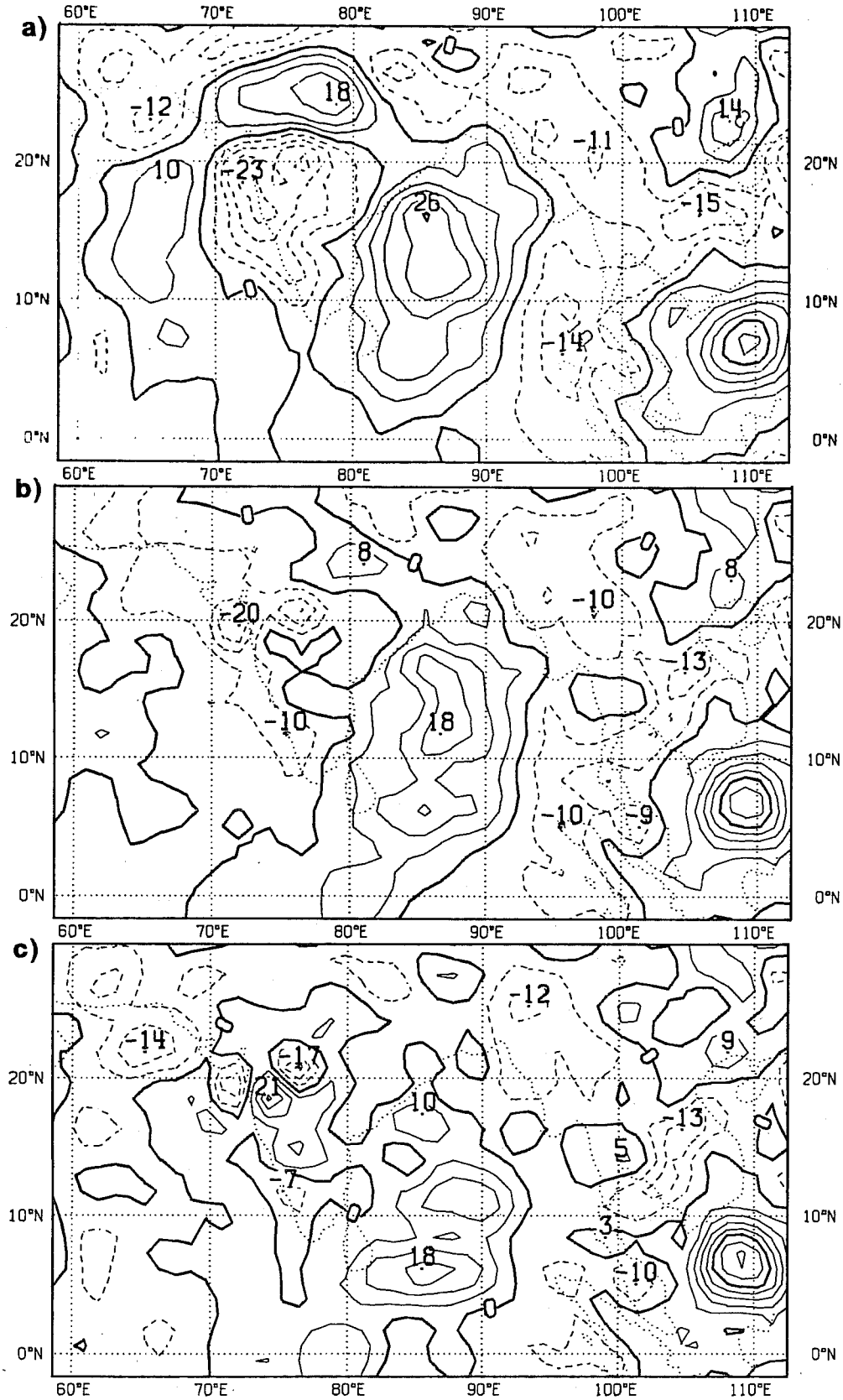

Figure 20. Analysis increments of divergence at 200 hPa 870822 12 UTC when analysing with the divergent structure functions (a,top) and with the divergent ones using twice the length scale as for the rotational part (b,below). The operational non-divergent analysis increments are shown in (c). Unit is 10^{-6} s^{-1} and isolines are for every $5*10^{-6}$ s^{-1}.

7. CONCLUSIONS

Inclusion of divergent terms in the ECMWF OI analysis is rather straight-forward and the impact on the wind analysis can be quite remarkable in terms of drawing to the data as already shown by Daley (1985). Instead of introducing the divergence in a very indirect and noisy way through data selection the inclusion of divergent terms makes the analysis increments of divergence smooth and laterally consistent.

Wind analyses are much improved locally in the tropics which is evident at any time when enough data are available. Where the non-divergent analysis is very poor the divergent one produces a rather reasonable wind field considering the scales resolved by the analysis. Also in a statistical sense there is evidence of better use of the wind data since the RMS-fits are improved.

SATOB's provide most of the input for the strong divergent signals seen during the assimilation and though it is clear that much better use has been made of them there is a risk that they exaggerate the divergent component of the wind. This is of course difficult to verify since there are very few tropical TEMP/PILOT co-locations but from the ones seen in the examples during these assimilations there is a tendency for the SATOB winds to be stronger than the measured ones in the western tropical Pacific.

Although the divergent analysis increments are radically improved most of the divergence field itself comes from the first guess. No significant impact has been noted in terms of precipitation and heating rates in ensuing 6-hour forecasts. The signals introduced through the analysis including divergence survive initialisation rather well and although some effect may be seen in the first guess for the next analysis it then disappears in presence of data in analysis or otherwise in the next 6-hour forecast step.

The divergent structure functions improve the analysis significantly but the forecast impacts are very small and rather neutral in terms of medium range forecast scores. Just improving the divergent wind is not enough to radically alter forecast of the tropical convective systems but it must be a prerequisite for further work in the area of tropical data assimilation.

Acknowledgements

I am grateful to my colleagues at ECMWF for discussions and comments. In particular I am indebted to Dr. A. Hollingsworth for valuable suggestions and comments which improved the manuscript and pointed to some relevant points in the discussions of the subject.

References

Buell, C.E. 1972. Correlation functions for wind and geopotential on isobaric surfaces. J.Appl.Meteorol. 11,51-59

Daley, R. 1983. Spectral characteristics of the ECMWF objective analysis system. ECMWF Tech. Rep. No. 40,117pp, ECMWF, Shinfield Park, Reading, Berkshire RG2 9AX, England.

Daley, R. 1985. The analysis of synoptic scale divergence by a statistical interpolation scheme. Mon.Wea.Rev. 113,1066-1079

Hollingsworth, A. 1984. Meteorological data analysis. Lecture Note No. 2.2 Chapt. 6, ECMWF, Shinfield Park, Reading, Berkshire RG2 9AX, England.

Hollingsworth, A., Shaw, D.B., Lonnberg, P., Illari, L., Arpe, K. and Simmons, A. 1986. Monitoring of observations and analysis quality by a data assimilation system. Mon.Wea.Rev. 114,861-879

Hollingsworth, A. and Lonnberg, P. 1986. The statistical structure of short-range forecast errors as determined from radiosonde data. Part I: The wind field. Tellus 38A,111-136

Lorenc, A. 1979. Meteorological data analysis. Lecture Note No. 3, 68 pp. ECMWF, Shinfield Park, Reading, Berkshire RG2 9AX, England.

Lorenc, A. 1981. A global three-dimensional multivariate statistical interpolation scheme. Mon.Wea.Rev. 109,701-721

Lonnberg, P. and Hollingsworth, A. 1986. The statistical structure of short-range forecast errors as determined from radiosonde data. Part II: The covariance of height and wind errors. Tellus 38A,137-161

National Research Council 1985. Procedures of the First National Workshop on the Global Weather Experiment, Woods Hole, Massachusets, USA, 1984. National Academy Press.

Pedder, M.A. 1988. On the influence of map analysis formulation in the estimation of wind field derivatives. Q.J.R.Meteor.Soc. 114,241-257

Shaw, D.B., Lonnberg, P., Hollingsworth, A. and Unden, P. 1987. Data assimilation: The 1984/85 revisions of the ECMWF mass and wind analysis. Q.J.R.Meteor.Soc. 113,533-566

Wergen, W. 1987. Diabatic nonlinear normal mode initialisation for a spectral model with a hybrid vertical coordinate. ECMWF Tech.Rep. No. 59,117pp, ECMWF, Shinfield Park, Reading, Berkshire RG2 9AX, England.

Unden, P. 1984. Evaluation of analysis increments at model levels. ECMWF Res.Dept. Tech.Memo. No. 94 25pp, ECMWF, Shinfield Park, Reading, Berkshire RG2 9AX, England.